

1
2
3
4
5
6
7 **Cultivating advanced embryo models through bioengineering mastery**

8
9 Xufeng Xue¹, Yue Liu¹, and Jianping Fu^{1, 2, 3 *}

10
11 ¹Department of Mechanical Engineering, University of Michigan, Ann Arbor, Michigan, USA;

12 ²Department of Biomedical Engineering, University of Michigan, Ann Arbor, Michigan, USA;

13 ³Department of Cell & Developmental Biology, University of Michigan Medical School, Ann Arbor,
14 Michigan, USA.

15
16 *Correspondence should be addressed to J.F. (email: jpfu@umich.edu)

17 **ABSTRACT**

18 Stem cell-based embryo models, which recapitulate symmetry breaking, pattern formation and tissue
19 morphogenesis during early development, provide promising experimental tools to study development
20 of mammalian species, including humans. Despite considerable progress in embryo modeling using
21 cultured stem cells, it remains challenging to construct embryo models with high fidelity, efficiency,
22 controllability, and *in vivo*-like cellular organization and tissue architecture. This is largely due to
23 intrinsic variabilities in self-organization and differentiation of mammalian stem cells in uncontrolled
24 culture environments utilized in current embryo modeling. In this review, we argue that bioengineering
25 tools, which are powerful for controlling topological boundaries and dynamic chemical and mechanical
26 signals and thus are efficient in guiding symmetry breaking, pattern formation, tissue morphogenesis
27 and tissue-tissue interactions, should be utilized for constructing high-fidelity, high-efficiency embryo
28 models. In this review, we first discuss pattern formation and morphogenesis during embryonic
29 development, and selectively examine different embryo models to highlight the importance of
30 bioengineering controls in developing these models. We then explore how different bioengineering
31 approaches useful for guiding pattern formation, morphogenesis, cell fate decisions and cell-cell
32 interfaces can be utilized in stem cell-based embryo modeling to promote their efficiency,
33 reproducibility, controllability, complexity, and *in vivo* relevance.

34

35 **1. INTRODUCTION**

36 During development, patterned multicellular structures with stereotypical, three-dimensional tissue
37 architecture emerge from a single fertilized egg. Mammalian development involves coordinated
38 developmental processes, including pattern formation, tissue morphogenesis, cell differentiation, and
39 growth¹. Pattern formation establishes body axes in mammalian embryos, including anterior (head)-
40 posterior (tail) (A-P) and dorsal (back)-ventral (belly) (D-V) axes. Mammalian embryos undergo
41 substantial morphological changes in form, or morphogenesis, to achieve complex tissue and organ
42 anatomies. Mammalian development also encompasses cell differentiation, giving rise to specialized cell
43 types with tissue- or organ-specific functions, and tissue growth. These developmental processes are
44 intricately linked during dynamic, progressive development. Precisely how the mammalian embryo
45 develops from a fertilized egg through these coordinated developmental processes remains one of the
46 most fundamental questions in biology with enormous biomedical implications.

47 Recent advances in stem cell biology, developmental biology and bioengineering have fostered
48 the emergence of an exciting interdisciplinary field termed stem cell-based embryo modeling²⁻⁵. This
49 field aims to apply developmental biology principles to create embryo models using mammalian
50 pluripotent and extraembryonic stem cells *in vitro*. When differentiated *in vitro*, these stem cells largely
51 follow the natural developmental programs of their *in vivo* counterparts⁶. Over the last decade, numerous
52 studies have showcased the intrinsic self-organizing properties of these cells to differentiate and self-
53 assemble into embryonic- or extraembryonic-like structures *in vitro* (see examples discussed in two
54 excellent reviews^{7,8}). Thus, stem cell-derived embryo models have successfully been developed to
55 recapitulate major developmental processes such as tissue patterning and morphogenetic events during
56 the pre-implantation, gastrulation, neurulation, and somitogenesis^{3,4,9} (**Table 1**). Nonetheless, continuous
57 development and future applications of stem cell-based embryo models hinge on the premise that these

58 models can serve as useful experimental tools to disentangle the genetic, molecular and cellular events
59 involved in human embryogenesis.

60 Given their high tractability and ease with which mammalian stem cells can be genetically
61 modified, stem cell-based embryo models have been hailed as promising experimental tools for studying
62 mammalian development and associated disorders^{3,10,11} (**BOX 1**). However, despite considerable
63 excitement and success in these models, they have rarely been used to reveal fundamental new insights
64 into mammalian development or in translational applications. One major hindrance to such important
65 applications of embryo models is that it remains a significant challenge for these models to faithfully
66 recapitulate tissue patterning or morphogenetic events occurring in natural embryonic development (or
67 fidelity) with a sufficiently high level of successful rate (or efficiency). This difficulty arises largely
68 because approaches for embryo modeling have been heavily relying on spontaneous differentiation and
69 self-organization of mammalian stem cells and their progenies in uncontrolled culture environments.
70 Consequently, their developments are critically affected by stochastic genetic noises or random cellular
71 interactions with local culture microenvironment. Genetic noises, which arise from stochastic variations
72 in the synthesis and degradation of mRNA and proteins¹², could contribute to phenotypic variabilities
73 observed in embryo models. Random interactions between stem cells using in embryo modeling and
74 their local microenvironment could further compound the efficiency or fidelity of embryo models¹³.

75 So far, a variety of mammalian stem cells, including pluripotent stem cells (PSCs) and stem cells
76 of extraembryonic lineages, such as trophoblast stem cells (TSCs)^{14,15} and extraembryonic endoderm
77 cells (XENs)¹⁶, have been utilized for building embryo models. However, culture conditions for these
78 stem cells have not yet been standardized. Furthermore, human extraembryonic stem cells remain to be
79 fully established. Additionally, human PSCs (hPSCs) generated using different culture protocols might
80 represent distinct pluripotency states with varied differentiation potentials¹⁷. These variabilities of

81 mammalian stem cells used in embryo modeling further complicate robust development and,
82 consequently, limit the usefulness and broad applications of embryo models in fundamental or
83 translational applications.

84 In this review, we aim to highlight bioengineering tools and their promising applications for
85 constructing high-efficiency and high-fidelity embryo models. Bioengineering approaches developed
86 over the last few decades are powerful in designing synthetic cells to regulate their responses to external
87 stimuli or controlling dynamic external microenvironmental signals critical for cellular behavior and fate
88 regulation¹³. In this review, we first discuss the two prominent developmental processes involved in
89 embryonic development: pattern formation and morphogenesis. We selectively examine different
90 embryo models, each clearly manifesting one or more of these embryonic developmental processes, with
91 an emphasis on the importance of bioengineering controls implemented in their development. We then
92 discuss how bioengineering approaches for guiding pattern formation, morphogenesis, cell fate
93 decisions and cell-cell interactions can enable precise control of the formation and development of
94 embryo models, enhancing their efficiency, reproducibility, complexity and *in vivo* relevance. We
95 conclude by discussing the limitations of current embryo models before highlighting design principles
96 that should be considered to promote the widespread applications of stem cell-based embryo models.
97

98 **2. PATTERN FORMATION**

99 In development, pattern formation is the process by which cellular activity is organized both spatially
100 and temporally such that a well-ordered tissue structure develops¹⁸. Pattern formation can be either self-
101 organized¹⁹ or guided by external cues²⁰. Self-organized pattern formation involves patterning of cell
102 fates through spontaneous cell-cell interactions among a seemingly homogeneous cell population¹⁹. One
103 such system, proposed by Alan Turing, is based on the reaction-diffusion model, in which stable patterns

104 emerges *via* cell-cell interactions through diffusion of activator-inhibitor pairs²¹. Turing's reaction-
105 diffusion model has successfully explained pattern formation in various *in vivo* (e.g., hair follicle
106 patterning²²) and *in vitro* (e.g., two-dimensional or 2D gastrulation models²³) contexts. The initial and
107 boundary conditions of pattern formation morphogenetic fields are critical for generating a reproducible
108 pattern in self-organized pattern formation¹⁹. As such, bioengineering approaches effective in
109 controlling initial cell number and geometries of cell colonies have been used for generating robust
110 embryo models whose developments rely on self-organized pattern formation^{24,25}.

111 For external cue-guided pattern formation, spatially patterned cell fates are instructed by external
112 signals, such as diffusible molecules, including both morphogens and their antagonists, secreted from
113 adjacent pre-formed tissues that function as signaling centers. External cue-guided pattern formation can
114 be explained by the positional information theory proposed by Lewis Wolpert²⁶. This theory proposes
115 that concentrations of external morphogens provide positional values as in a coordinate system for cell
116 fate decisions²⁶. Recent studies, however, also support the important roles of other features of
117 morphogen gradients (gradient slope, duration and time integral) in providing positional information for
118 spatial cell fate patterning^{27,28}. It should be noted that morphogen gradients can also arise through
119 intrinsic cell-cell interactions per Turing's reaction-diffusion model, which then provides positional
120 information to guide pattern formation. For example, a stepwise reaction-diffusion and positional model
121 was proposed to explain pattern formation in 2D human gastrulation models²⁹. There are effective
122 bioengineering approaches for controlling exogenous soluble culture environments, such as
123 bioengineered co-culture systems for controlling paracrine signals and microfluidic devices for
124 generating dynamic morphogen gradients^{13,30}. Importantly, such bioengineering tools have been
125 successfully employed in embryo models to recapitulate external cue-guided pattern formation³¹⁻³⁴.

126 Even though pattern formation *in vivo* often involves both self-organized cell-cell interactions

127 and external cue-guided spatial fate patterning³⁵, there are some well-studied pattern formation events in

128 development in which each of these mechanisms plays an essential role. In this section, we first discuss

129 three such events and related embryo models successfully developed to recapitulate them: 1)

130 Specification of trophectoderm (TE), hypoblast and epiblast (EPI) during blastocyst formation through

131 self-organized pattern formation, 2) A-P symmetry breaking in the EPI at the onset of gastrulation

132 guided by extraembryonic tissues, and 3) neural tube (NT) patterning *via* morphogen gradients. We next

133 discuss how bioengineering approaches have been implemented in embryo models to enhance the

134 efficiencies of recapitulating these pattern formation events by guiding cell-cell interactions and

135 controlling external bio-physical and -chemical signals.

136

137 **2.1. Pattern formation *in vivo* and in embryo models**

138 *Blastocyst formation and modeling through self-organized pattern formation.* The first major symmetry

139 breaking event in mammalian development takes place during blastocyst formation^{36,37}. During

140 blastocyst development, cells of the morula undergo an ordered series of cell-fate decisions and

141 symmetry-breaking events. This developmental sequence results in the formation of a blastocyst,

142 composed of TE surrounding the blastocoel and inner cell mass (ICM) (**Fig. 1a**). After implantation, the

143 TE contributes to placental development. Within the blastocyst, the ICM differentiates into two distinct

144 cell lineages: EPI, forming the embryo proper, and hypoblast, or called primitive endoderm (PrE) in

145 mice (**Fig. 1a**).

146 Most of the current knowledge about lineage segregations during blastocyst formation comes

147 from studies of mouse embryos. We now know that lineage segregation between TE and ICM cells

148 occurs first during blastocyst formation. At the 8-cell stage, driven by cortical tension, the mouse

149 embryo becomes compacted, and each individual cell acquires an apical domain³⁸ (**Fig. 1a**). As mouse
150 morula cells divide, cells in the outer layers inherit apical components and become polarized, whereas
151 those in inner layers become apolar³⁹ (**Fig. 1a**). The distinct polarity status leads to differential Hippo
152 signaling and subsequent differential expression of TE- and EPI-related transcription factors in the outer
153 and inner cells of the mouse morula to specify TE and EPI fates, respectively^{40,41}. Thus, embryo
154 geometry, coupled with cortical tension, cell position, and division pattern, defines the polar to apolar
155 cell ratio and thus TE and ICM lineage allocation^{38,42-44} (**Fig. 1a**). After TE and ICM lineage bifurcation,
156 transmembrane pumps in TE cells pump fluids into extracellular space in the mouse blastocyst, leading
157 to formation of small fluid-filled cavities⁴⁵. These cavities coalesce into a single large cavity, the
158 blastocoel, due to pressure imbalance⁴⁶. After blastocoel formation, ICM cells become segregated into
159 EPI and PrE^{36,37}. Specification of EPI and PrE in mice is regulated by heterogeneous FGF signals in the
160 ICM, with EPI precursors secreting FGF ligands to drive PrE fate specification in neighboring cells⁴⁷
161 (**Fig. 1a**). Thus, PrE and EPI cells initially form a “salt-and-pepper” pattern, before cell sorting to
162 establish a well delineated spatial pattern of PrE and EPI cells, with PrE layer lining the blastocoel and
163 EPI surrounded by PrE and TE⁴⁸. Molecular mechanisms underlying human hypoblast development
164 remain elusive. There are two studies showing that FGF inhibition does not have a significant effect on
165 hypoblast induction in human blastocysts^{49,50}. However, more recent studies suggest that FGF inhibition
166 could suppress specification of hypoblast or hypoblast-like cells in human blastocysts or from naïve
167 hPSCs, respectively^{51,52}. Thus, additional studies are needed to reconcile these discrepancies to fully
168 elucidate the role of FGF signaling in human hypoblast specification.

169 Stem cell-based models of blastocysts, or blastoids, were first generated using mouse stem
170 cells⁵³⁻⁵⁵ (**Fig. 1b, Table 1**). Since then, numerous human blastoid systems have been reported^{24,56-60}
171 (**Fig. 1b, Table 1**). Human blastoids resemble human blastocysts in terms of morphology, transcriptome

172 and lineage composition. Given the potency of naïve hPSCs for both embryonic and extraembryonic
173 lineage developments⁶¹, they have been the most commonly used starting cell populations for
174 developing human blastoids^{24,58,59,61}. Regardless the initial cell types being used, human blastoid
175 protocols commonly involve seeding and aggregating hPSCs in confining microwell plates to initiate
176 and promote self-organized tissue patterning^{24,56,58-61}. In such blastoid formation protocols, initial cell
177 number in each cell aggregate, which is controlled by cell seeding density, appears to be an important
178 factor affecting blastoid formation^{24,58,61}. Low cell numbers in initial aggregates of hPSCs often lead to
179 formation of trophoblast spheroids lacking ICM-like cells⁶¹. How the initial cell number in hPSC
180 aggregates affects human blastoid formation remains unclear. After initial cell aggregate formation, cell
181 clusters are then exposed to ERK, ROCK and NODAL inhibitors to induce TE lineage
182 differentiation^{24,58,59,61}. Similar to TE and ICM lineage segregation during human blastocyst
183 development, the outer and inner cells in human blastoids acquire differential polarity status and Hippo
184 signaling activity, leading to the outer and inner cells being specified into TE-like and ICM-like cells,
185 respectively^{24,58,59,61}. Notably, similar to natural human blastocyst development, inhibition of Hippo
186 signaling promotes TE differentiation and increases the efficiency of human blastoid generation^{24,59}.
187 Although hypoblast-like cells are present in human blastoids, they are not as developed or organized as
188 their *in vivo* counterpart. This deficiency underscores our current limited understanding of human
189 hypoblast lineage development.

190 Given that human blastoids can be generated with high efficiency (~ 80%) and in large
191 quantities, they offer a useful experimental tool to study human pre- and peri-implantation development.
192 For example, there are implantation modeling studies by co-culturing human blastoids with endometrial
193 epithelial cells and stromal cells^{24,59,62}. These studies support that in human blastoids maturation of TE
194 cells and their interaction with endometrial epithelial cells are both regulated by signals emanated from

195 EPI-like cells²⁴. The presence of endometrial stromal cells also seems to promote progressive
196 development of human blastoids into early peri-implantation stages⁵⁹.

197

198 *Epiblast symmetry breaking during peri-gastrulation development and its modeling.* After implantation,
199 the next major milestone of mammalian development is the gastrulation, through which the single layer
200 of pluripotent EPI cells transforms into a multilayered and multidimensional structure with fully defined
201 body axes. Human gastrulation remains mysterious. Current knowledge about mammalian gastrulation
202 is mainly derived from studies of mouse embryos, revealing the important role of extraembryonic tissues
203 in inducing symmetry breaking of the EPI and establishing the A-P axis at the onset of gastrulation³⁶.
204 Specifically, in pre-gastrulation mouse egg cylinder, the EPI is surrounded by the extraembryonic
205 ectoderm (ExE) derived from TE and visceral endoderm (VE) derived from PrE. Regionalized BMP
206 signals from the ExE leads to formation of a distal VE (DVE) at the distal region of VE^{63,64} (**Fig. 1c**).
207 Involving NODAL and WNT signaling, DVE subsequently migrates towards one side of the embryo
208 and specifies into anterior VE (AVE), thereby marking the future anterior domain of mouse embryos⁶⁵
209 (**Fig. 1c**). The AVE secrets WNT, NODAL and BMP antagonists, shielding anterior EPI from
210 posteriorization and thus restricting the primitive streak formation and gastrulation to posterior EPI^{66,67}
211 (**Fig. 1c**).

212 In contrast to a cup shape of the pre-gastrulation mouse EPI, pre-gastrulation human EPI exhibits
213 a disc-like morphology, and it is juxtaposed with the dorsal amniotic ectoderm and ventral hypoblast⁶⁸
214 (**Fig. 1c**). How the amniotic ectoderm and hypoblast regulate symmetry breaking and the A-P axis
215 formation in the EPI during human gastrulation remains unclear. Recent studies of *in vitro* cultured
216 human embryos reveal a portion of hypoblast cells at the putative anterior region expressing BMP, WNT
217 and NODAL antagonists^{69,70}, similar to the mouse AVE. Nonetheless, whether these cells act as the

218 anterior signaling center to induce symmetry breaking and establish the A-P axis in the human EPI
219 remains to be fully elucidated.

220 Stem cell-based embryo models that recapitulate symmetry breaking and the formation of A-P
221 axis in the EPI offer promising tools to study these important developmental events and the underlying
222 genetic, molecular and cellular mechanisms. Towards this goal, peri-gastrulation mouse embryo models
223 have been generated by aggregating mouse embryonic stem cells (mESCs) and mouse TSCs (mTSCs) in
224 3D Matrigel culture⁷¹ (**Table 1**). Through spontaneous self-organization, some cell aggregates formed
225 organized egg cylinder-like structures, termed ESC- and TSC-derived embryo model, or ETS embryo
226 model⁷¹. ETS embryo model comprises mESC-derived pseudostratified EPI-like epithelium juxtaposed
227 with mTSC-derived ExE-like cells⁷¹. Even though lacking VE-related lineages, some ETS embryo
228 models could undergo symmetry breaking and give rise to regionalized mesoderm tissues⁷¹. How this
229 occurs in ETS embryo models without VE-related lineages is unclear, possibly depending on genetic
230 noises or random cellular interactions with local culture microenvironments. Whether such a mechanism
231 plays a role in symmetry breaking and A-P patterning of the mouse EPI *in vivo* warrants future
232 investigation. Follow-up studies incorporated mouse XENs, the *in vitro* counterpart of PrE, into ETS
233 embryo models, resulting in a more complete peri-implantation mouse embryo model, termed ETX
234 embryo models (ESC-, TSC-, XEN-derived embryo models)^{72,73} (**Fig. 1d, Table 1**). A-P patterning was
235 also achieved in ETX embryo models, evidenced by the development of AVE-like cells expressing
236 signaling antagonists and graded expression of NODAL in posterior EPI-like cells^{72,73}. ETX embryo
237 models further exhibited cellular features of the gastrulation, including epithelial-mesenchymal
238 transition (EMT) of the EPI and formation of mesoderm and endoderm lineages^{72,73}. Both ETS and ETX
239 embryo models show limited efficiencies (20 - 30%) due to random, uncontrolled interactions between
240 embryonic and extraembryonic cells in the models⁷¹⁻⁷³. Notably, the ETX embryo model presents the

241 potential for development beyond gastrulation (**Table 1**). To this end, *in vitro* studies of natural embryos
242 are very useful in guiding the culture protocol development for stem cell-based embryo models. When
243 cultured in an *ex utero* mouse embryo roller culture system under optimized medium conditions⁷⁴, ETX
244 mouse embryo models develop structures mimicking the neural tube (NT), heart, gut tube, somites and a
245 tail bud, albeit with a very low efficiency and organ primordia exhibiting notable defects⁷⁵⁻⁷⁷.

246 Recently, assembloid approaches have been utilized for scalable and controllable generations of
247 peri-gastrulation mouse embryo models^{31,78} (**Table 1**). Assembloids are 3D structures formed through
248 fusion of two or multiple spheroids to recapitulate structural and functional properties of an organ^{79,80}.
249 Assembloids are instrumental in modeling tissue-tissue interactions. However, due to its simplistic
250 assembly process, assembloids might be limited in modeling the complex tissue cytoarchitecture formed
251 through dynamic pattern formation processes in natural embryos. To model peri-gastrulation mouse
252 development, mESC and mTSC spheroids were assembled to guide their interaction, leading to the
253 formation of regionalized mesodermal cells in mESC spheroids with an efficiency of 50 - 70%⁷⁸.
254 Similarly, assembling of mESC clusters and BMP4-treated mESC clusters, which served as an
255 engineered signaling center secreting WNT and NODAL signals, resulted in peri-gastrulation mouse
256 embryo models showing well-delineated orthogonal A-P and D-V body axes and patterned germ layer
257 lineages with a efficiency greater than 90%³¹. Progressive development of this mouse embryo model
258 showed organ primordia similar to those in neurula-stage mouse embryos, including the NT, gut tube,
259 somitic and intermediate mesodermal tissues, cardiac tissues, and a vasculature network³¹. These
260 examples highlight how bioengineering approaches can be applied to control embryonic-extraembryonic
261 interactions to improve the efficiency of peri-gastrulation embryo model development.

262 Peri-gastrulation human embryo models were first developed from primed hPSCs without
263 involving extraembryonic cells⁸¹⁻⁸³ (**Table 1**). In one model exhibiting drastic symmetry breaking

264 events, a subset of primed hPSC clusters in 3D Matrigel culture spontaneously underwent epithelialization
265 and lumenogenesis, giving rise to a luminal epithelial structure, before spontaneously breaking
266 symmetry to form a bipolar structure mimicking early post-implantation EPI and amniotic ectoderm
267 patterning⁸³. This model was termed post-implantation amniotic sac embryoid (PASE)⁸³. Some of the
268 PASE structures progressively developed, with the EPI-like compartment undergoing EMT and giving
269 rise to mesodermal lineages⁸³. Follow-up studies using controllable microfluidic devices to provide
270 asymmetric external morphogen stimulations to primed hPSC clusters showed significantly enhanced
271 efficiencies of PASE formation³². Further mechanistic studies identified the role of paracrine signaling,
272 likely involving BMP signals downstream of *ISL1*, from amniotic cells in inducing gastrulation-like
273 events in the EPI at the onset of human gastrulation^{32,84}. This finding was further corroborated from
274 studies of peri-gastrulation primate monkey embryos⁸⁴.

275 Recently, there have been numerous peri-gastrulation human embryo models reported that
276 incorporated both embryonic and extraembryonic compartments, such as a yolk sac-like structure and
277 TE derivatives⁸⁵⁻⁹¹ (**Fig. 1d, Table 1**). Some of these models showed evidence suggesting that yolk sac
278 endoderm-like cells might secrete BMP and WNT antagonists to promote anterior ectoderm formation in
279 these models⁸⁵⁻⁹¹, supporting the notion that in humans there are yolk sac endoderm cells functioning
280 similarly as the mouse AVE to induce symmetry breaking and A-P patterning of peri-gastrulation human
281 EPI. Even though these recently reported human embryo models are promising for studying embryonic-
282 extraembryonic interactions in the peri-gastrulation human development, their limited efficiencies in
283 modeling EPI symmetry breaking and A-P patterning and forming *in vivo*-like tissue structures remain a
284 significant issue. Continuous efforts will be needed to improve the efficiencies of these models to
285 promote their applications for fundamental studies to understand tissue-tissue interactions and patterning
286 in human development.

287

288 *Morphogen-mediated NT patterning and its modeling.* During gastrulation, embryonic germ layer
289 subpopulations in the mammalian embryo come together, facilitating interactions that shape tissue
290 layers, specify cell types, and initiate organ rudiment development. A critical event in the embryonic
291 ectoderm after gastrulation is the NT formation and patterning, laying the foundation of the functional
292 complexity and anatomical organization of the human nervous system. Patterning of NT along the A-P
293 axis leads to the formation of four main NT subdivisions: forebrain, midbrain, hindbrain and spinal cord
294 (**Fig. 1e**). D-V patterning of each NT subdivision gives rise to various neuronal progenitor cells along
295 the D-V axis. For example, D-V patterning of the spinal cord results in the formation of eleven neural
296 progenitor domains - 5 ventral and 6 dorsal – each expressing a specific combination of transcription
297 factors that constrain their lineage development.

298 Knowledge of NT patterning mostly comes from studies of chick and mouse embryos. It is well
299 established that axial patterning of NT involves external morphogen gradients, which establish
300 positional information across the NT along both the A-P and D-V axes. A-P patterning is mainly
301 governed by P-A gradients of posteriorizing signals including WNT, retinoic acid (RA) and FGF⁹²⁻⁹⁴
302 (**Fig. 1e**). A-P patterning of the NT is further refined by developmental signals emanated from
303 secondary organizers, such as FGF signals from the anterior neural ridge and the isthmic organizer at the
304 midbrain-hindbrain boundary⁹⁵ (**Fig. 1e**). D-V patterning of the NT is mainly mediated by antiparallel
305 gradients of BMP / WNT and SHH along the D-V axis^{96,97} (**Fig. 1e**). BMP and WNT molecules are
306 secreted by dorsal non-neural ectoderm and subsequently by the roof plate, whereas SHH is emanated
307 from the ventral notochord and subsequently by the floor plate^{96,97} (**Fig. 1e**). RA secreted from the
308 paraxial mesoderm and somites flanking the NT is also important for ventral patterning of the NT⁹⁸.

309 Stem cell-based NT patterning models have been successfully established with both mESCs and

310 hPSCs, leveraging their self-organizing pattern formation properties⁹⁹⁻¹⁰¹ (**Table 1**). Seeded in Matrigel

311 or synthetic poly(ethylene glycol) (PEG)-based hydrogels under neural induction culture conditions,

312 both mESCs and hPSCs formed spherical luminal neuroepithelial cysts containing a single central

313 lumen⁹⁹⁻¹⁰¹. When ventralizing signals RA and / or SHH were supplemented into culture medium, D-V

314 patterning of neuroepithelial cysts was evident, featuring sequential emergence of the ventral floor plate,

315 P3, and pMN domains in discrete, adjacent regions and a dorsal territory progressively restricted to the

316 opposite dorsal pole^{99,100}. It remains unclear how global applications of exogenous ventralizing

317 morphogens lead to self-organized, D-V patterning of neuroepithelial cysts. Experimental data showed

318 that at the initial phase of D-V patterning, FOXA2+ floor plate progenitor cells emerged first in

319 neuroepithelial cysts, but in a scattered fashion^{99,100}. Soon thereafter, FOXA2 expression became

320 restricted to a local floor plate-like region, defining the ventral pole of neuroepithelial cysts^{99,100}. It was

321 suggested that this FOXA2+ floor plate-like domain might function as a local signaling center to induce

322 and pattern other ventral regions in both the mouse and human neuroepithelial cysts^{99,100}. Further

323 mechanistic studies revealed that self-organized D-V patterning of mouse neuroepithelial cysts might

324 involve interactions of BMP and Noggin with a reaction-diffusion-based Turing patterning

325 mechanism^{102,103}. Whether such self-organized patterning mechanisms operate *in vivo* for axial

326 patterning of the NT is unclear. PEG-based hydrogel systems with tunable degradability, stiffness and

327 matrix composition were also utilized in D-V patterning of mouse neuroepithelial cysts to disentangle

328 the contributions of individual biochemical and physical components of the microenvironment¹⁰¹.

329 Nevertheless, D-V patterning of mouse and human neuroepithelial cysts under uniform culture

330 conditions remains inefficient.

331 Microfluidics technologies, which can provide precise spatiotemporal controls of chemical
332 signals, have been successfully implemented to create morphogen environments for different neural
333 tissue engineering applications, including improving patterning efficiency of stem cell-based NT
334 development models^{33,34} (**Table 1**). For example, D-V patterned human forebrain organoids derived
335 from hPSCs were generated by culturing embryonic bodies under a SHH gradient generated in a passive
336 diffusion-based microfluidic gradient generator¹⁰⁴. Another microfluidic device that employed a series
337 of splitting and mixing of microfluidic flows was utilized to generate a linear WNT signal gradient
338 across 2D layers of hPSCs³³. This microfluidic device was shown effective in generating an A-P
339 patterned human NT development model that exhibited progressive caudalization from forebrain to
340 midbrain to hindbrain³³. Interestingly, an isthmic organizer-like domain spontaneously emerged in this
341 human NT model between the midbrain- and hindbrain-like regions, thus highlighting the autonomous
342 and self-organizing properties of NT development, leading to the formation of local secondary
343 organizers at NT subdivision boundaries³³.

344 More recently, we reported a hPSC-based, microfluidic NT-like structure (or μ NTLS), whose
345 development recapitulated some critical aspects of human neural patterning in both the brain and spinal
346 cord regions and along both A-P and D-V axes in a 3D tubular geometry³⁴ (**Table 1**). To generate A-P
347 and D-V patterned μ NTLS, tubular-shaped hPSC tissues were generated in a microfluidic chamber, in
348 which morphogen gradients were established through passive diffusion of different morphogens added
349 to medium reservoirs connected to the chamber. Orthogonal morphogen gradients were established, one
350 of WNT, RA and FGF8 signals along the length of μ NTLS to induce its A-P patterning and the other of
351 antiparallel BMP4 and RA / SHH signals perpendicular to the μ NTLS length to induce its D-V
352 patterning (**Fig. 1f**). Importantly, the μ NTLS was utilized for studying neuronal lineage development,
353 revealing pre-patterning of axial identities of neural crest progenitors and functional roles of

354 neuromesodermal progenitors (NMPs) in spinal cord and trunk neural crest development. Thus, stem
355 cell-based NT development models, developed using microfluidic tools with an *in vivo*-like
356 spatiotemporal cell differentiation and organization, are promising for studying human
357 neurodevelopment and disease.

358

359 **2.2. Bioengineering tools to guide pattern formation**

360 As discussed, pattern formation can be either self-organized¹⁹ or guided by external cues²⁰. Self-
361 organized pattern formation depends on spontaneous cell-cell and cell-microenvironment interactions,
362 whereas for external cue-guided pattern formation, precisely controlled dynamic external signals, such
363 as diffusible molecules, are of critical importance. Bioengineering approaches that are efficient in
364 controlling cell number and geometries of morphogenetic fields, tissue-tissue interactions (including
365 both paracrine and juxtacrine interactions), and external chemical gradients are of most significant
366 relevance to improve the efficiency and fidelity of modeling tissue patterning using stem cells *in vitro*.

367

368 *Controlling initial cell cluster formation.* Commercial AggreWell and micropatterned agarose microwell
369 plates have been utilized in blastoid and other embryo model developments, including ETS and ETX
370 embryo models^{24,56,58-61,71-73} (**Fig. 2a**). These microwell plates are useful for improving the efficiency
371 and throughput of these embryo models, since confining microwell environments promote cell
372 aggregation and cell-cell interactions. However, microwell plates have some notable limitations. Firstly,
373 AggreWell only allows control over the size but not the geometry of initial cell aggregates. This issue
374 can be addressed by using 3D hydrogel microwells fabricated by molding or laser ablation of hydrogels
375 such as collagen or Matrigel^{105,106}. In this way, the initial cell cluster geometry can be fully defined by
376 the hydrogel microwell shape. The pyramidal shape of AggreWell also prevents high-quality *in situ*

377 imaging of embryo models. High-resolution imaging of free-floating embryo models requires two-
378 photon light sheet microscopy. Microfluidics, which is compatible with high-quality *in situ* imaging,
379 provides an alternative approach to control initial cell cluster formation for embryo modelling. For
380 developing the PASE, microfluidics was used to precisely control the size and location of hPSC clusters
381 with defined cell numbers by aggregating hPSCs in preformed concave hydrogel pockets³². Using the
382 microfluidic PASE system, live imaging was conveniently conducted to track tissue morphogenetic
383 events, including symmetry breaking, and signaling dynamics using reporter lines³².

384 In development, pattern formation is often followed by tissue growth and organ functional
385 maturation. Microfluidic tools, even though convenient for controlling the formation of initial cell
386 clusters and their positions in prescribed locations inside microfluidic environments, are intrinsically not
387 ideal for long-term culture and continuous growth of embryo models. It is foreseeable that future
388 developments of this direction would involve integrated applications of microfluidics and conventional
389 tissue cultures to promote long-term growth of spatially patterned embryo models, with initial cell
390 cluster formation and tissue patterning conducted in microfluidic devices, followed by transferring
391 embryo models to conventional culture systems for continuous development and tissue growth.

392
393 *Bioengineered co-culture systems to guide tissue-tissue interactions.* A successful co-culture system
394 should satisfy three key criteria: 1) the system should allow precise controls of the proportions of each
395 cell type within specific regions of the co-culture, 2) the co-culture system should allow efficient cell-
396 cell interactions (paracrine or juxtacrine interactions), and 3) the culture environment should facilitate
397 co-culturing of different cell types. The last criterion relies on improved knowledge from stem cell
398 biology and developmental biology. The first two criteria, however, could benefit from the development
399 and application of bioengineering approaches.

400 Micropatterning-based co-culture platforms, which rely on PDMS stencils or microcontact
401 printing, have been well developed to precisely control spatiotemporal organizations of two or more
402 different adherent cell types in 2D cultures¹⁰⁷⁻¹¹⁰. Stencil-based co-culture platforms, however, are
403 unable to physically separate distinct cell types¹⁰⁸⁻¹¹⁰, making it unsuitable for decoupling juxtacrine and
404 paracrine interactions. In contrast, microcontact printing-based co-culture methods could control the
405 distance between different cell types, rendering them suitable for studying paracrine interactions¹⁰⁷.
406 There are also micromachined silicon substrates with controllable moving parts to dynamically control
407 tissue organization and composition through mechanical repositioning, thus enabling investigations of
408 dynamic cell-cell interactions¹¹¹. This micromachined silicon substrate system was successfully applied
409 to investigate intercellular communication in co-cultures of hepatocytes and non-parenchymal cells¹¹¹.
410 Owing to their superior controllability and compatibility with live imaging, these 2D co-culture
411 platforms show considerable promise for generating advanced 2D embryo models to study tissue-tissue
412 interactions. Micropatterning-based co-culture platforms are also compatible with many other
413 microengineering and mechanobiology tools, such as microfluidic gradient devices¹¹², tissue stretching
414 devices¹¹³, microfabricated pillar force sensor arrays¹¹³, and surface biosensing techniques¹¹⁴. Integrated
415 applications of these bioengineering tools will enable control, perturbation and quantification of both
416 bio-chemical and -physical factors involved in tissue-tissue interactions during embryo modeling. For
417 example, amnion has been suggested to function as a signaling center secreting BMP and/or WNT
418 molecules to drive the primate gastrulation^{32,84}. However, the molecular mechanism(s) underlying the
419 amnion-EPI interaction remains unconfirmed, and it is difficult if not impossible to use primate
420 embryonic tissues for such mechanistic investigations. An amnion-EPI co-culture model can be
421 developed using micropatterning-based co-culture methods to study the role and nature of their
422 interactions in driving primate gastrulation. Additionally, integration of such 2D amnion-EPI co-culture

423 platforms with surface biosensing techniques could provide concrete information about paracrine or
424 juxtacrine interactions between the two tissues during primate gastrulation. Direct measurements of
425 BMP and WNT ligands, in combination with genetic and chemical perturbations, in the amnion-EPI co-
426 culture model could shed light on molecular mechanism(s) underlying inductive effects of amnion on
427 human EPI development.

428 2D co-culture platforms are limited to studying intercellular and tissue-tissue communications in
429 2D settings. Transitioning from 2D to 3D cell culture, 3D bioprinting is emerging as a promising
430 technology to control and study tissue-tissue communications in 3D settings. 3D bioprinting allows
431 precise and flexible assembly of living cells, tissues, biomaterials, and other bioactive factors into
432 complex 3D structures, replicating the intricate architecture of biological tissues or organs¹¹⁵ (**Fig. 2b**).
433 Even though 3D bioprinting has not yet been applied for embryo modelling, it has been utilized for the
434 development of some promising high-cell density heterogeneous tissue models¹¹⁶. For example,
435 magnetic- and aspiration-assisted bioprinting is one of the embedded 3D bioprinting methods that uses
436 aspiration forces to transfer tissue spheroids into self-healing support hydrogels at high resolution, which
437 enables their patterning and fusion into high-cell density microtissues of prescribed spatial
438 organization^{117,118} (**Fig. 2b**). This bioprinting method was recently applied to develop co-cultures of
439 hPSC-derived cardiomyocytes and cardiac fibroblasts to recapitulate structural and functional features of
440 cardiac tissues¹¹⁷. In another example of embedded 3D bioprinting, perfusable vascular channels were
441 printed into large quantities of organ-specific spheroids to promote their long-term growth and
442 maturation¹¹⁹.

443 We envision that controllable and reproducible tissue co-culture platforms with prescribed
444 spatial tissue organizations, based on either 2D systems or 3D bioprinting, will have immense potentials
445 for building advanced embryo models that could be utilized for advancing our understanding of

446 intercellular communications and tissue-tissue interactions in human development, which remains very
447 difficult to study.

448

449 *Engineering signaling centers and morphogen gradients.* Chemical signals, often in the form of
450 signaling molecules such as growth factors and morphogens, guide cellular behaviors, ensuring proper
451 organization and specialization of cells for the formation of functional tissues and organs during
452 development. Understanding and manipulating chemical signals are fundamental to studying
453 developmental biology and hold important implications for advanced embryo modeling. *In vitro*
454 methods for spatiotemporal control of chemical signals involve various techniques to precisely
455 manipulate the distribution and timing of signaling molecules in cell culture environments. These *in*
456 *vitro* methods include chemical-soaked microbeads^{120,121}, microfluidics^{30,122,123}, engineered morphogen-
457 secreting signaling centers^{31,124,125}, and optogenetics^{126,127} (**Fig. 2c**).

458 Chemical-soaked beads are often used in developmental biology studies to create controlled
459 microenvironments and study the effects of localized chemical signals and their gradients on developing
460 tissues or organisms. Porous beads are loaded with growth factors, hormones or morphogens, before the
461 beads are placed near developing tissues or embryos. Passive diffusion of chemicals loaded in the beads
462 leads to the formation of their local gradients, allowing studies of how the presence of specific
463 chemicals and their varying concentrations influence cell behaviors including cell fate changes (**Fig. 2c**).
464 Chemical-soaked microbeads were used successfully in studying morphogen-guided pattern formation
465 in amphibian embryos^{128,129}. In a recent study, CHIR- and BMP-soaked agarose beads were placed
466 adjacent to human brain organoids to induce localized dorsal cortical hem-like identities in the
467 organoids¹²⁰.

468 Localized signaling centers can also be generated by engineering cells either chemically or
469 genetically. Since treating mESCs with BMP4 upregulates *Nodal* and *Wnt3* expression in the cells,
470 clusters of BMP-treated mESCs could serve as a signaling center emanating NODAL and WNT signals.
471 Assembly of BMP-treated mESC clusters with wild-type mESC clusters led to the development of an
472 mouse embryo model that recapitulated the formation and organization of the three embryonic germ
473 layers³¹ (**Fig. 2c**). In another study, genetically modified, chemically inducible SHH-secreting hPSCs
474 were placed on one side of human brain organoids. Under chemical induction, these modified hPSCs
475 secreted SHH to guide patterning of human brain organoids to form spatially restricted forebrain
476 subregions, including regions resembling the ganglionic eminence, hypothalamus, thalamus and dorsal
477 forebrain¹²⁴.

478 Chemical-soaked beads and engineered signaling centers can easily be adopted in biological labs
479 owing to their simplicity. However, it is difficult to precisely control the range, slope and temporal
480 dynamics of morphogen gradients using these methods, thus limiting quantitative studies of morphogen
481 signals and their roles in pattern formation and other developmental processes. These limitations can be
482 addressed by using microfluidics. Microfluidics can control spatiotemporal distributions of signaling
483 molecules and thus create signaling gradients with precise ranges and slopes (**Fig. 2c**). As discussed
484 earlier, a linear microfluidic WNT signal gradient was utilized to generate an A-P patterned human NT
485 model³³. D-V patterned human forebrain organoids were generated by culturing embryoid bodies under
486 a linear SHH gradient in microfluidic devices¹⁰⁴. Another advantage of microfluidics is its versatilities
487 and capabilities for different bioengineering applications, including generating 3D orthogonal
488 morphogen gradients useful for inducing A-P, D-V, medial-lateral and left-right patterning along the
489 three body axes. As discussed earlier, we recently developed a microfluidic device that could establish
490 two orthogonal morphogen gradients through passive diffusion of morphogens in a microfluidic

491 chamber³⁴ (**Fig. 2c**). A-P and D-V patterned μ NTLS were generated by exposing hPSC-derived tubular
492 neuroepithelial tissues to such orthogonal morphogen gradients in the microfluidic chamber³⁴.

493 Despite its technical versatility and precision in controlling morphogen dynamics, microfluidics
494 remains challenging to be adopted in common biology and biomedical research laboratories. This is
495 mainly due to the fact that microfluidic device design and fabrication can be complex and require
496 specialized knowledge in microfabrication techniques. The intricate structures and precise features
497 necessary for microfluidic functionalities can also be challenging to produce and troubleshoot.

498 Biological laboratories may not always have personnel with the diverse skill set needed to design,
499 fabricate and operate microfluidic systems. Efforts are being made to address these challenges through
500 the development of user-friendly microfluidic platforms, improved standardization, and increased
501 collaboration between engineers and biologists^{30,130}. As microfluidic technologies continue to advance
502 and mature, it is likely that some of these barriers will be overcome, making microfluidic devices more
503 accessible and widely adopted in biological laboratories for stem cell research and embryo modeling.

504 Optogenetics is another useful approach for establishing exogenous morphogen gradients. Some
505 optogenetic approaches have been developed to enable photoactivation of transcription factors for
506 controlling gene expression with high spatiotemporal precision, and as such are promising for generating
507 localized signaling centers by inducing subpopulations of cells in a large cell population to produce
508 specific morphogen signals¹³¹ (**Fig. 2c**). Compared to microfluidics, potentially more precise temporal
509 control over morphogen signals can be achieved using optogenetics. Local activation of SHH through
510 optogenetics in a human spinal cord organoid was shown to robustly induce spatially organized ventral
511 spinal cord domains surrounding SHH secreting cells^{126,132}. Nonetheless, there are still some important
512 technical limitations of optogenetic approaches for transcriptional controls, including off-target effects,
513 limited tissue penetration, phototoxicity and limited dynamic range¹³³. Optimization and validation steps

514 are crucial for obtaining reliable and interpretable results using optogenetic approaches for
515 transcriptional controls.

516 We envision that advances in different bioengineering approaches, particularly those based on
517 microfluidics and optogenetics, and continued refinement of existing systems to precisely control
518 spatiotemporal dynamics of chemical environments and cellular signaling, will enable the development
519 of more advanced and sophisticated embryo models that can faithfully and reproducibly model pattern
520 formation as well as progressive tissue development.

521

522 **3. TISSUE MORPHOGENESIS**

523 Proper morphogenesis processes are required for tissues and organs to acquire their 3D structures during
524 development. Morphogenesis is achieved by coordinated cellular activities, such as cell division,
525 adhesion, migration, and changes in cell shape. Cell-cell adhesive interactions maintain tissue
526 boundaries and enable tissue-level cell arrangements and movements. Loss of cell-cell adherens
527 junctions between epithelial cells leads to EMT, as in the primitive streak formation during
528 gastrulation¹³⁴. The formation of adherens junctions between mesenchymal cells results in their
529 epithelialization; this process, termed mesenchymal-to-epithelial transition (MET), is involved in
530 condensation and segmentation of presomitic mesoderm (PSM) to form somites¹³⁵. *In vitro*, cell-cell
531 adhesions can be engineered using synthetic biology approaches to facilitate tissue assembly to build
532 multicellular structures (see Section 4 for more discussions). Cell shape change and cell migration,
533 which are regulated by dynamics of the intracellular cytoskeleton, are crucial in many morphogenetic
534 events, such as the gastrulation and neurulation^{134,136}. Cell shape can be modulated by geometrical
535 confinement (e.g., micropatterning) and mechanical perturbations (e.g., tissue stretching)^{25,113}. These
536 bioengineering approaches have been applied to build embryo models such as 2D micropatterned

537 gastrulation and neural development models and to study the roles of cell mechanics and the
538 cytoskeleton in embryonic development^{25,113}.

539 Cell-ECM interactions play crucial roles in tissue morphogenesis by influencing cell shape,
540 polarity and organization^{137,138}. Cell-ECM interactions are also essential for cell migration during
541 processes such as the gastrulation and organogenesis^{137,138}. Besides providing mechanical support and
542 promoting tissue integrity, cell-ECM interactions modulate various signaling pathways, influencing
543 processes such as proliferation, survival and differentiation^{137,138}. There are recent studies in which
544 different embryo models were embedded in natural or synthetic hydrogels; this step was critical for
545 triggering morphogenetic events mimicking neurulation and somitogenesis, supporting the importance
546 of controlling cell-ECM interactions in modeling proper tissue morphogenesis in embryo modeling¹³⁹⁻
547 ¹⁴¹. Over the last decade, there has been remarkable progress in developing various embryo and organ
548 models that recapitulate key morphogenetic events during mammalian development.

549

550 **3.1. Morphogenesis *in vivo* and in embryo models**

551 *Gastrulation: forming organized body plan.* As a highly orchestrated process, gastrulation lays the
552 foundation of the basic body plan^{36,68,134}. Besides germ layer lineage fate specification, gastrulation
553 involves a myriad of morphogenetic events to organize the topology of the three definitive germ layers.
554 These morphogenetic events include EMT, cell migration, convergent extension, and elongation along
555 the A-P axis^{134,142} (**Fig. 3a**). Much attention has been paid to mimicking germ layer lineage
556 differentiation and patterning in peri-gastrulation embryo models established using 2D micropatterned
557 hPSC colonies treated with exogenous BMP4²⁵ (**Fig. 3b, Table 1**). These 2D human gastrulation
558 models are compatible with live imaging and can be generated robustly, thus allowing quantitative
559 mechanistic studies of how self-organized signaling events drive lineage fate patterning during

560 gastrulation. Several signaling mechanisms were identified using these 2D micropatterned human
561 gastrulation models, including dynamic waves of BMP, WNT and NODAL signaling, interaction of
562 endogenous activators and inhibitors in a diffusion-reaction mechanism, and basolateral localization of
563 BMP receptors^{23,28,29}. The latter mechanism was further shown to play a role in the formation of a robust
564 BMP signaling gradient in peri-gastrulation mouse embryos¹⁴³.

565 3D gastrulation models, or gastruloids, have been generated by treating 3D clusters of mESCs or
566 hPSCs with a pulse of WNT agonist CHIR99021, leading to the formation of an A-P axis and
567 differentiated germ layer derivatives spatially organized along this axis^{139,144-146} (**Table 1**). More
568 advanced gastruloids were demonstrated to recapitulate the formation of organ primordia during early
569 organogenesis, such as the NT, bilateral somites, gut tube, and cardiac tissues, by optimizing chemical
570 and mechanical signals in gastruloid culture environments^{141,147,148} (**Table 1**). Tissue organization and
571 patterning in gastruloids were achieved without the presence of extraembryonic lineages, suggesting
572 self-organized pattern formation mechanisms in play. Recently, numerous post-implantation and peri-
573 gastrulation human embryo models that incorporated putative extraembryonic signaling centers, such as
574 the amnion, yolk sac and TE derivatives, were reported⁸⁵⁻⁹¹ (**Table 1**). These models are promising for
575 studying how self-organized patterning mechanisms function synergistically with embryonic-
576 extraembryonic interactions to ensure the robustness of the gastrulation process and embryonic germ
577 layer organization.

578 There is emerging evidence suggesting that cell fate patterning and morphogenesis are possibly
579 regulated independently during gastrulation^{134,149}. This observation is corroborated by findings from 2D
580 micropatterned gastrulation models and gastruloids, which recapitulate spatially patterned cell fate
581 organization during gastrulation but with limited morphogenetic events. However, how cell fate
582 patterning and morphogenesis are coordinated to establish the body plan during gastrulation remains ill-

583 understood. Stem cell-based embryo models that can mimic both cell fate patterning and morphogenetic
584 events during gastrulation are thus promising for elucidating this important question.

585 To promote morphogenetic events, bioengineering approaches have been integrated with
586 gastrulation models. For example, culturing micropatterned 2D human gastrulation models on a soft
587 polyacrylamide hydrogel that recapitulated the biophysical properties of early embryos promoted a
588 “gastrulation-like” morphogenesis of hPSCs, including self-organization of “gastrulation-like” nodes
589 and ingress and migration of mesoderm cells through the nodes¹⁵⁰ (**Fig. 3b, Table 1**). This study
590 further showed that tissue geometries dictated the formation of “gastrulation-like” nodes in regions
591 where high cell-adhesion tension would arise, which directed spatial patterning of BMP4-dependent
592 “gastrulation-like” phenotype by promoting WNT signaling and mesoderm specification. Further
593 integration of this micropatterned 2D human gastrulation model with a bioengineered tissue stretching
594 device showed that direct force application *via* mechanical stretching could promote BMP-dependent
595 mesoderm specification¹⁵⁰, confirming the role of tissue-level forces in directly regulating lineage
596 differentiation during gastrulation^{151,152}.

597 Without the presence of extraembryonic tissues, there is no structure formation in gastruloids
598 that mimics the primitive streak^{142,146}. Other morphogenetic events associated with the gastrulation,
599 including collective cell migration, also don’t seem to occur in gastruloids^{142,146}. However, when mESCs
600 were co-cultured with extraembryonic cells such as mTSCs and/or XENs in ETS and ETX embryo
601 models, a primitive streak-like structure emerged in the compartment of mESCs adjacent to mTSCs⁷²
602 (**Table 1**). Similarly, in a 3D human peri-gastrulation model encompassing both embryonic and
603 extraembryonic tissues, a putative primitive streak-like structure emerged at the posterior end of the
604 model, characterized by cells at this region undergoing EMT and inward migration¹⁵³ (**Table 1**).
605 Together, these studies suggest that the primitive streak might be a transient structure whose formation

606 involves the mechanics and geometrical boundary constraints imposed by adjacent extraembryonic
607 tissues^{134,142}. Using bioengineering approaches to control tissue mechanics and topology as well as cell-
608 cell and cell-ECM interactions during embryo modeling will be an important direction to recapitulate
609 and study morphogenetic events that occur during the gastrulation.

610 One morphogenetic event that is well recapitulated in gastruloids is axial elongation. Along the
611 A-P axis, peri-gastrulation embryo elongates, with progenitors in the tail bud proliferating and
612 differentiating to give rise to tissues that generate posterior spinal cord, skeleton and musculature¹⁵⁴. In
613 gastruloids, posterior progenitors, likely including NMPs, emerge at their posterior ends^{139,141,144-146}.
614 These cells have been shown to give rise to both neural and mesodermal lineages and contribute to
615 posterior elongation of gastruloids^{139,141,144,145}. In mouse gastruloids, P-to-A gradients of Erk and Akt
616 signals were shown to play important roles in controlling the unidirectional tissue growth at their
617 posterior ends by modulating cell proliferation, motility and adhesion¹⁵⁵. Tissue elongation and
618 narrowing along the A-P axis, which resembles convergent extension during mouse gastrulation, was
619 also observed in mouse gastruloids¹⁵⁶. Consistently, an *in silico* model showed that convergent extension
620 could help explain the elongation of gastruloids¹⁵⁶. In embryonic development, convergent extension is a
621 conserved complex process involving a series of molecular and cellular events that coordinate cell
622 movements and rearrangements, including cell polarization, dynamic changes of cell adhesion and
623 cytoskeleton, cell intercalation, and planar cell polarity signaling¹⁵⁷. It will be important for future
624 studies to examine whether similar molecular and cellular events are involved in axial elongation of
625 mouse and human gastruloids.

626
627 *Neurulation: tissue bending morphogenesis.* Neurulation describes the developmental process through
628 which the NT is formed from the neural plate (NP) specified in the ectoderm. After gastrulation, the

629 ectoderm is specified into the neuroectoderm, containing the NP, flanked by the neural plate border
630 (NPB) and non-neural ectoderm (NNE), through the process of neural induction. As the neurulation
631 progresses, the NP undergoes structural changes, with the lateral edges of the plate elevating to form two
632 parallel ridges called neural folds (**Fig. 3c**). The neural folds eventually meet in the dorsal midline of the
633 embryo and fuse to form the hollow NT, containing a central lumen called neural canal (**Fig. 3c**). In
634 mammals, NP bending is primarily driven by mechanical forces generated by apical constriction in NP
635 cells at the median and dorsolateral hinge points¹³⁶ (**Fig. 3c**). There is also evidence suggesting the role
636 of proliferation of NNE tissues in generating mechanical pushing forces to facilitate NP bending and
637 closure¹³⁶. Once the two opposing neural folds meet at the dorsal midline, cells at the tips of the neural
638 folds develop cellular protrusions to attach to the opposite neural folds. The NT then becomes separated
639 from the dorsal NNE tissue due to differential adhesions.

640 Neurulation is a tightly regulated process, disruption of which can lead to NT closure defects
641 (NTDs), one of the most common congenital disorders affecting the nervous system. Genetic mutations
642 affecting BMP, SHH, WNT, and planar cell polarity signaling pathways, impaired cell proliferation,
643 apoptosis and ECM formation, abnormal cell adhesion, migration and actomyosin turnover, oxidative
644 stress and inflammation, and environmental factors have all been implicated in NTDs¹⁵⁸⁻¹⁶¹. Dynamics
645 of the neurulation depends on the A-P axial level¹³⁶. Fusion of neural folds begins in the middle of the
646 embryo and moves anteriorly and posteriorly¹³⁶. Disruption of several actin-associated proteins prevents
647 bending of the NP only in anterior regions but not in spinal regions¹⁶¹⁻¹⁶⁴, supporting different dynamics
648 and regulatory mechanisms of the neurulation at different A-P axial levels. Understanding the molecular
649 and cellular mechanisms underlying neurulation is pivotal for providing insights into the etiology of
650 NTDs. Most of the knowledge about neurulation comes from studies of chick and mouse embryos,
651 which remains to be validated in human-relevant models. Recently, various stem cell-based human

652 neurulation models have been developed using hPSCs^{113,140,165-168} (**Table 1**). These models offer
653 accessible and tractable experimental tools to study different morphogenetic events involved in human
654 neurulation.

655 The luminal morphology of human NT was initially modeled successfully using 2D neural
656 rosettes containing a single central lumen^{165,169} (**Table 1**). Neural rosettes are 2D neuroepithelial tissues
657 derived from hPSCs. The initial tissue geometry of 2D neural rosettes plays an important role in lumen
658 formation. Thus, using micropatterning tools to control the geometry of 2D neuroepithelial tissues,
659 neural rosettes with a single lumen were derived reproducibly from hPSCs with a high efficiency¹⁶⁵.
660 More recently developed 2D micropatterned neurulation models using hPSCs recapitulated
661 neuroectoderm patterning and even the single lumen morphology of the NT^{113,166,167} (**Table 1**). Studies
662 using these models demonstrated the important roles of both bio-mechanical and -chemical cues in
663 neuroectoderm patterning^{113,166,167}. Importantly, these studies further supported the self-organization of
664 morphogenetic cues, including cell shape and cytoskeletal contractility, in neuroectoderm patterning¹¹³.
665 Self-organized morphogenetic cues could directly feedback to mediate BMP activity to guide spatial
666 regulation of neuroectoderm patterning¹¹³. Thus, mechanistic studies of neuroectoderm patterning using
667 these 2D micropatterned neurulation models support intricate patterning signaling crosstalk involving
668 both biophysical and biochemical determinants, which may be important in controlling patterning
669 networks to ensure the remarkable robustness and precision of neuroectoderm patterning *in vivo*.

670 Since 2D micropatterned neurulation models are confined to 2D surfaces, they are intrinsically
671 not suitable for recapitulating the dynamic NP folding process during neurulation, which might limit
672 their applications for studying NTDs. A recent study combining micropatterned 2D hPSC colonies with
673 3D culture successfully recapitulated neuroectoderm patterning followed by the dynamic NP folding and
674 fusion process, leading to the formation of a 3D tubular structure mimicking the cranial NT with a high

675 efficiency¹⁴⁰ (**Fig. 3d, Table 1**). This 3D human neurulation model was further utilized for modeling
676 NTDs, specifically demonstrating the impacts of chemicals perturbing apical constriction and basal
677 ECM synthesis on folding and closure of the NP.

678 Spinal cord organoids derived from hPSCs have also been reported that recapitulate neurulation-
679 like tube-forming morphogenesis of the early spinal cord¹⁶⁸ (**Table 1**). Specifically, to develop these
680 spinal cord organoids, caudalized 2D hPSC colonies, likely through a transient NMP stage, were
681 detached from 2D cultures to form 3D spheroids in a free-floating culture. These spheroids were induced
682 with a neuroepithelial fate. NP-like structures spontaneously emerged at the surfaces of these 3D
683 spheroids, and they underwent folding morphogenesis to form NT-like structures within the 3D
684 spheroids, likely involving apical constriction in neuroepithelial cells¹⁶⁸. Neurulation-like tube-forming
685 morphogenesis in the spinal cord organoids occurred in the absence of NPB or NNE tissues, supporting
686 a role of innate self-organizing properties of NP cells in driving their folding dynamics¹⁶⁸.

687
688 *Somitogenesis: tissue segmentation morphogenesis.* Somitogenesis is the process by which somites are
689 formed in the embryo. Somitogenesis establishes the segmented pattern of the vertebrate body plan,
690 essential for proper formation and function of the musculoskeletal system. Defects or disruptions in
691 somitogenesis lead to congenital abnormalities such as scoliosis. Current knowledge about
692 somitogenesis is mainly derived from chick and mouse studies. During somitogenesis, the PSM, a
693 bilateral strip of mesenchymal tissue flanking the forming NT, progressively segments into bilaterally
694 symmetrical epithelial somites in the A-P direction¹³⁵ (**Fig. 3e**). Somitogenesis can be explained by the
695 clock-and-wavefront model, which proposes that somitogenesis is regulated by the combined action of a
696 molecular clock mechanism within the PSM and a moving wavefront of signaling activity along the A-P

697 axis¹³⁵ (**Fig. 3e**). This model provides a conceptual framework for understanding how the periodic
698 segmentation of somites is controlled during embryonic development.

699 Somitogenesis has provided an excellent model to study the formation of morphological
700 boundaries between developing tissues. New somites are formed at the anterior end of the PSM, where
701 cells undergo MET and coalesce into a rosette-like structure that pulls apart from the PSM. Specifically,
702 cells in forming somites at the anterior PSM undergo rearrangements, which involves changes in cell
703 adhesion, cell shape and cell-cell interactions, contributing to the morphological formation of an
704 intersomitic boundary (also called a fissure) and separation of forming somites from the PSM¹⁷⁰. Fissure
705 formation in somitogenesis has been suggested as an intrinsic property of PSM cells and does not rely
706 on surrounding tissues¹⁷¹. After its formation, PSM cells in the somite undergo MET, resulting in the
707 conversion of loosely packed mesenchymal cells into tightly packed epithelial cells, which contribute to
708 the structural integrity of somite boundaries¹⁷⁰. Besides classic morphogenetic studies of the
709 somitogenesis, recent studies revealed decreasing cell stiffness, polarity, and adhesion along the A-P
710 axis in the chick PSM¹⁷². Applying external mechanical stress along the A-P axis of the chick PSM also
711 induced the formation of new somite boundaries that were not determined by the clock-and-wavefront
712 model, suggesting mechanical cues could be instructive for somite formation^{173,174}.

713 Somitogenesis was first recapitulated in gastruloids. When embedded in Matrigel, mouse
714 gastruloids, termed trunk-like structures, developed a NT-like structure flanked by the PSM and
715 epithelial somite-like tissues¹⁴¹ (**Fig. 3f, Table 1**). Recently, similar human somitogenesis models were
716 developed by culturing hPSC clusters in PSM differentiation environments¹⁷⁵⁻¹⁷⁸ (**Table 1**). These
717 models exhibited oscillatory expression of clock genes in the PSM, the periodic segmentation and
718 epithelialization of somites, and A-P polarity of each single somite. Novel biological insights into
719 somitogenesis were revealed from these models, including an unexpected role of cell sorting during

720 somite formation and the role of RA in epithelialization of somites^{177,178}. Matrigel appeared to be critical
721 for epithelialization of somitic cells but was not required for somitic differentiation of PSM cells in
722 either mouse or human somitogenesis models, highlighting the importance of the ECM environment in
723 morphogenetic events involved in somitogenesis^{141,177,178}.

724 To study the biochemical-biomechanical interactions that drive somitogenesis, another
725 somitogenesis model was recently developed in a microfluidic device by controlling exogenous anti-
726 parallel RA and WNT / FGF signaling gradients and mechanical boundaries in hPSC-derived PSM
727 tissues¹⁷⁹ (**Table 1**). A fracture mechanics-based theoretical model, which considered strain energy
728 induced by compaction of a forming somite and surface energy resulted from a new somite-PSM
729 boundary, was proposed to explain the role of mechanics in regulating somite size. Despite its simplistic
730 nature, this theoretical model revealed a scaling law connecting the dimension of nascent somite with
731 the length of PSM. The primary correlation between nascent somite sizes and the PSM length agreed
732 with data from mouse, chick, zebrafish and human embryos quantitatively, supporting a common
733 mechanics-based mechanism in play in regulating somite boundary formation in different species.

734 Co-morphogenesis of NT- and somite-like structures was also achieved in mouse and human
735 trunk-like structures, under a low dose of WNT signal stimulation^{141,180} (**Fig. 3f, Table 1**). *In vivo*,
736 posterior NT and somites originate from a common caudal progenitor population, including NMPs.
737 Mouse and human trunk-like structures, recapitulating the spatiotemporal development of these three
738 lineages, could be very useful for studying their lineage relationships and the genetic and molecular
739 mechanisms underlying caudal lineage diversifications.

740

741 **3.2. Bioengineering tools to guide morphogenesis**

742 During development, morphogenesis is brought about by the coordination of intra- and inter-cellular
743 forces and their interactions with surrounding tissues and ECM. Intracellular forces are generated by the
744 contractile cytoskeleton, which are transmitted to the local cell microenvironment through cell-cell and
745 cell-ECM adhesions. Surrounding tissues and ECM with specific geometries and mechanical and
746 biochemical properties provide additional boundary conditions that can influence tissue morphogenesis.
747 Through both *in vivo* and *in vitro* studies, it has become clear that the geometrical tissue boundary
748 conditions provide a ground state for morphogenetic events^{134,142}. Thus, bioengineering approaches
749 effective in controlling geometrical boundaries of 2D and 3D tissues are useful for engineering tissue
750 morphogenesis and improving the efficiency and robustness of embryo and organ model developments.
751 Furthermore, synthetic biomaterials engineered with specific mechanical properties and / or
752 functionalized with growth factors and signaling molecules can be promising for guiding tissue
753 development and organization in embryo models. In this section, we discuss bioengineering approaches
754 for controlling geometrical boundaries of 2D and 3D tissues and different biomaterial systems for
755 embryo models. Discussions of synthetic biology approaches to control intracellular contractility and
756 cell-cell and cell-ECM adhesions are in Section 4.

757

758 *Engineering tissue geometry and boundary.* Micropatterning allows the creation of 2D cell colonies with
759 controlled size, shape, and physical boundary conditions. In micropatterning, patterns of adhesive
760 molecules at the micro- and nanoscale resolutions are created on 2D tissue culture surfaces (either tissue
761 culture plates or glass coverslips) through a variety of bioengineering tools, including microcontact
762 printing¹⁸¹, stencil micropatterning^{182,183}, and photopatterning²⁵ (**Fig. 4a**). Thus, selective adhesion of
763 mammalian cells to micropatterned adhesive regions leads to formation of 2D cell colonies with
764 prescribed sizes and shapes (**Fig. 4a**).

765 Microcontact printing, the process to print adhesive islands onto substrates using stamps, is
766 currently the most widely used technique to generate micropatterned 2D cell colonies in cell biology and
767 tissue engineering laboratories¹⁸¹. In microcontact printing, adhesion properties, surface energy, and
768 chemical compatibility between the stamp, printed adhesive molecules and substrates must be carefully
769 considered to ensure successful pattern transfer. Furthermore, stamp reusability and surface
770 homogeneity can be issues. In microcontact printing, stamps are often generated using microfabrication,
771 which requires access to cleanroom facilities, thus limiting wide applications of this convenient and
772 powerful technology in biology and biomedical research laboratories.

773 Stencil micropatterning involves the use of stencils, which are essentially masks with specific
774 patterns or designs cut out of them. These stencils are placed onto a substrate, and material is deposited
775 or removed through the openings in the stencil to create desired patterns on the underlying surface.
776 Thus, in stencil micropatterning, the stencil-to-substrate contact is important in determining pattern
777 fidelity and impacting experimental reproducibility. Stencil micropatterning was originally developed
778 for microelectronics applications^{184,185}. However, it has also found applications in generating
779 micropatterned 2D cell colonies by applying stencils onto cell culture substrates before cell
780 seeding^{182,183}. After cell seeding, stencils can be removed to release geometrical constraints to the
781 growing cell colonies, to promote their long-term development. Stencil micropatterning is best suited for
782 simple geometric patterns with well-defined shapes and features. Similar to microcontact printing,
783 stencil micropatterning typically provides static, fixed patterns on substrates. The lack of dynamic
784 control over pattern geometry and cell behaviors limits the applicability of stencil micropatterning and
785 microcontact printing for certain tissue engineering studies.

786 In photopatterning, cell culture surfaces coated with a layer of cytophobic or cell-repellent
787 molecules are patterned using UV light passing through a photomask¹⁸⁶⁻¹⁸⁸. Localized UV light exposure

788 of cytophobic molecules promotes their degradation and exposes underlying cell culture surfaces for
789 subsequent functionalization with adhesive molecules to promote local cell attachment¹⁸⁶⁻¹⁸⁸. Similar to
790 microcontact printing and stencil micropatterning, photopatterning typically involves patterning cells at
791 a single time point, resulting in static, fixed patterns. Photopatterning also relies on the use of
792 photosensitive materials whose long-term cytotoxic effects and degradation properties need to be
793 carefully evaluated. Nonetheless, micropatterned cell culture surfaces generated using photopatterning
794 are commercially available, which promotes broader applications of micropatterning techniques for 2D
795 cell culture studies, especially in research labs that lack access to microfabrication tools²⁵.

796 3D morphogenetic events cannot be fully recapitulated in 2D cell culture systems. Nonetheless,
797 integration of 2D micropatterning tools and 3D culture expands the application of 2D micropatterning to
798 model 3D morphogenetic events, such as tissue folding and fusion¹⁴⁰. In addition, 3D structures made of
799 PDMS or hydrogels containing channels or wells of defined sizes and shapes, which are fabricated by
800 soft lithography or laser ablation, have also been utilized for guiding morphogenetic events involved in
801 the somitogenesis and intestinal morphogenesis^{105,106,179} (**Fig. 4a**). Given their superior reproducibility,
802 scalability, and compatibility with live imaging, micropatterned 2D or 3D culture systems are promising
803 for translational applications such as drug and toxicity screens.

804

805 *Bioengineering hydrogels.* *In vivo*, the ECM provides structural support, mechanical stability, and
806 biochemical signaling cues for guiding morphogenetic events during embryonic development. Matrigel,
807 a gelatinous protein mixture extracted from Engelbreth-Holm-Swarm mouse sarcoma, is the most
808 widely used natural ECM for 3D cultures, including embryo and organ model cultures. However,
809 Matrigel is ill-defined with significant batch-to-batch variations, which limits the reproducibility of 3D
810 cultures using Matrigel¹⁸⁹. In addition, Matrigel offers no direct control over its molecular composition

811 or components, making it unsuitable for studying the role of individual ECM components in regulating
812 embryonic development¹⁸⁹. Since Matrigel is derived from animals, there is a risk of contamination with
813 animal-derived factors, hindering clinical applications of Matrigel¹⁸⁹.

814 Over the last few decades, there have been tremendous advances in fully defined synthetic
815 biomaterials and their applications in 3D tissue cultures. By incorporating bioactive molecules, cell-
816 adhesive motifs, and tissue-specific cues into synthetic biomaterials, these synthetic biomaterials are
817 designed to mimic the structure and function of natural ECM. Synthetic matrices such as PEG-based
818 hydrogels have already been successfully utilized for reproducible development of mouse and human
819 intestinal organoids and D-V patterned mouse NT development models^{101,190-192}. Besides biochemical
820 properties, synthetic matrices also offer the advantageous feature of convenient and independent
821 modulations of their biophysical properties, such as degradability, porosity, and viscoelastic properties,
822 thus making them suitable for studying the independent effects of these factors on embryo and organ
823 model development^{101,190-192}. Systematically screening synthetic matrices of different properties will
824 lead to the discovery of optimal hydrogel conditions for the development and growth of embryo and
825 organ models, which will facilitate their scalable and reproducible production for both fundamental and
826 translational applications.

827 Another important future direction is to apply synthetic biomaterials with spatially patterned
828 biochemical and biomechanical properties, such as dynamically controllable growth factor release and
829 matrix stiffness changes, for guiding symmetry breaking, pattern formation, and morphogenesis of
830 embryo models^{138,193} (**Fig. 4b**). Hydrogels containing photoreversible immobilization of growth factors
831 were developed to achieve spatially localized growth and differentiation of human mesenchymal stem
832 cells¹⁹⁴⁻¹⁹⁶. Spatial patterning of cell adhesive ligands within 3D synthetic matrices was shown to guide
833 directional cell migration^{197,198}. Additionally, photo-induced hydrogel cross-link exchange reaction was

834 employed to spatiotemporally alter the local viscoelasticity of a synthetic hydrogel system formed
835 through reaction between PEG-dibenzylcyclooctyne and allyl sulfide bis(PEG3-azide). Photo-induced
836 local changes in the viscoelasticity of the hydrogel were utilized to control epithelial tissue curvatures
837 and study how dynamic changes in tissue curvatures influence mechanotransduction pathways to
838 instruct crypt morphogenesis in intestinal organoids¹⁹⁹. The spatiotemporal control of extracellular
839 signals, offered by such synthetic hydrogels, offer another layer of external regulation that can be
840 integrated with other bioengineering approaches, such as microfluidics and optogenetics, for future
841 development of controllable and programmable embryo models.

842

843 **4. ENGINEERING CELL FATE AND CELL-CELL INTERFACES USING SYNTHETIC 844 BIOLOGY**

845 Synthetic biology offers powerful molecular tools to design and construct new biological systems or
846 redesign existing biological systems for useful purposes. Over the last decade, synthetic biology
847 provides various approaches to control transcription factor expression, modulate signaling pathways,
848 manipulate epigenetic modifications, direct cell fate specification, and regulate cellular interactions and
849 organization²⁰⁰⁻²⁰³. Thus, synthetic biology offers attractive approaches orthogonal to microfluidics,
850 micropatterning and synthetic biomaterials to achieve programmable cellular complexity, architecture
851 and function in bioengineered embryo and organ models. Synthetic biology could contribute to the
852 construction of embryo models through engineering fate (**Fig. 5a**), engineering cell adhesion (**Fig. 5b**),
853 optogenetics (**Fig. 5c**), and engineering morphogen gradients (**Fig. 5d**). Optogenetics and bioengineered
854 signaling centers have been discussed in the section of “*Engineering signaling centers and morphogen
855 gradients*”. Thus, here we focus on discussing how transcription factor overexpression and synthetic cell

856 adhesions could be utilized for engineering cell fate and cell-cell interfaces, respectively, for improving
857 cellular complexity, composition and organization in embryo and organ models.

858

859 *Engineering cell fate.* Overexpression of transcription factors through genetic engineering has been
860 commonly employed for inducing cell differentiation or transdifferentiation (**Fig. 5a**). Compared with
861 chemical induction, transcription factor overexpression can produce specific cell lineages more quickly
862 and efficiently. Genetically engineering PSCs by overexpressing transcription factors could produce
863 additional cell sources for constructing embryo and organ models. As mentioned earlier, ETX embryo
864 models, developed by assembling mESCs, TSCs and XENs, resemble the mouse egg cylinder. ETX
865 embryo models, however, could not develop much further beyond the onset of gastrulation^{71,72} (**Table**
866 **1**). This limited developmental potential of ETX embryo model is likely resulted from heterogeneous
867 TSC and XEN populations, which contain subpopulations resembling different stages of their *in vivo*
868 counterpart development^{76,204}. When mouse TSCs and XENs were replaced with mESCs transiently
869 overexpressing *Cdx2* and *Gata4*, respectively, resulting mouse embryo models could progressively
870 develop beyond the gastrulation and reaching early organogenesis stages⁷⁵⁻⁷⁷, albeit with a very low
871 efficiency and containing organ primordia often showing notable structural defects (**Table 1**). More
872 recently reported, integrated peri-implantation human embryo models also utilized similar transcription
873 factor overexpression strategies to generate extraembryonic lineages, before assembling them with either
874 naïve or primed hPSCs for constructing peri-implantation human embryo models^{85,86,88-91} (**Table 1**).
875 These examples highlight the application of engineering cell fate through overexpressing transcription
876 factors to obtain homogenous stem cell or progenitor populations, promoting cellular complexity,
877 composition and organization in embryo models.

878 In another example, genetic engineering tools were combined with 3D bioprinting to construct
879 organoids with controlled cellular composition and organization. Specifically, an orthogonally induced
880 differentiation (OID) method was developed, by overexpressing different transcription factors in the
881 same hPSC population, to simultaneously differentiate the cells into various organ-specific lineages
882 independently of culture medium conditions²⁰⁵. This OID method was applied to generate endothelial
883 cells and neurons from hPSCs simultaneously under the same culture to produce vascularized cortical
884 organoids²⁰⁵. By integrating OID with multi-material bioprinting of hPSCs with inducible-transcription-
885 factor-overexpression, patterned neural tissues with layered regions composed of neural stem cells,
886 endothelium and neurons were generated, highlighting the promise of integrating 3D bioprinting and
887 orthogonally induced differentiation of stem cells for building multicellular tissue structures with
888 controlled cellular composition, organization and function²⁰⁵.

889

890 *Engineering cell adhesion.* Cell-cell adhesion is critical for tissue development by regulating tissue
891 architecture, cell behavior and signaling processes. Cadherins form adherens junctions between adjacent
892 cells, which play an important role in regulating tissue morphogenesis by maintaining tissue integrity,
893 shape and organization^{206,207}. Varying expression levels and types of cadherins could result in
894 autonomous cell sorting and segregation during tissue development, a phenomenon termed differential
895 adhesion²⁰⁷. Differential adhesion plays an important role in establishing tissue boundaries and spatial
896 organization during development^{206,207}. Interestingly, by overexpressing cadherin molecules specific to
897 the mouse EPI, TE and PrE in mESCs, TSCs and XENs, respectively, the efficiency of ETX embryo
898 model was improved through autonomous cell sorting and segregation similar to those in mouse
899 blastocyst formation²⁰⁸.

900 Over the past two decades, synthetic biologists have repurposed physical parts and concepts from
901 natural receptors to engineer synthetic receptors²⁰⁰. These technologies implement customized sense-
902 and-respond programs that link a cell's interaction with extracellular and intracellular cues to user-
903 defined responses, including rationally programmed assembly of multicellular architectures^{202,209} (**Fig.**
904 **5b**). In recent years, the library of synthetic receptors and their capabilities has substantially evolved. In
905 one recent study, synthetic cell adhesion molecules were demonstrated by combining orthogonal
906 extracellular interactions with intracellular domains from native adhesion molecules, such as cadherins
907 and integrins²⁰⁹. The resulting synthetic molecules were shown to yield customized cell-cell interactions
908 with adhesion properties that are similar to native interactions, including eliciting intracellular actin
909 cytoskeleton dynamics and tension²⁰⁹. How synthetic receptors could be utilized for improving the
910 efficiency of embryo and organ models remains to be demonstrated. This effort might further lead to the
911 development of programmable embryo and organ models endowed with certain enhanced
912 functionalities.

913

914 **5. PERSPECTIVE AND FUTURE DIRECTIONS**

915 In this review, we have discussed recent progress in stem cell-based embryo modeling and how
916 bioengineering approaches useful for engineering pattern formation and morphogenesis can be
917 employed to construct advanced embryo models with enhanced efficiency and controllability and
918 heightened cellular complexity, composition and organization. The heterogeneity of initial stem cell
919 populations used in embryo modeling and their less characterized functions are also important issues
920 that should be fully addressed. To this end, synthetic biology approaches to engineer cell fate have
921 shown significant promises to generate more uniform cell sources to construct embryo models.

922 Stringent validation of embryo models is important for their downstream applications, as how
923 faithfully an embryo model can recapitulate *in vivo* development determines its usefulness as a model
924 system to study embryo development. While it is desirable to compare embryo models with *in vivo*
925 embryos of the same species and compatible stages, this is a challenge when it comes to human embryo
926 modeling. Recent significant advancements in studies of *in vivo* and *ex vivo* cultured human and non-
927 human primate embryos provide important molecular and cellular knowledge for authenticating and
928 benchmarking human embryo models²¹⁰⁻²¹⁷. When comparing embryo models with *in vivo* or *ex vivo*
929 cultured embryos, we should not only consider molecular signatures, cell lineage identities or
930 multicellular tissue organization at isolated time points, but also examine the dynamic and progressive
931 tissue developmental events that cultivate their morphology, architecture and function.

932 Single-cell multiome, including single-cell RNA-sequencing (scRNA-seq), provides a wealth of
933 information about the molecular characteristics and functions of single cells, allowing researchers to
934 gain insights into cellular heterogeneity, cell-to-cell variability, and complex biological processes. Over
935 the past decade, numerous scRNA-seq datasets have been generated from *in vivo* and *ex vivo* cultured
936 human and non-human primate embryos at different development stages²¹⁴⁻²¹⁷. This rich information
937 provides important molecular references for authentication and identification of cell types,
938 characterization of their transcriptional states, detection of rare cell populations, and study of
939 intracellular signaling and tissue-tissue interactions in embryo models. When examining embryo models
940 and how useful they will be for fundamental and translational applications, great care must be taken to
941 understand the specific developmental stages and associated cell lineage developments each embryo
942 model is capable of recapitulating. There are many embryo models now available, with some considered
943 as integrated with both embryonic and extraembryonic compartments and others as non-integrated. For
944 many embryo models, there remains significant ethical challenges. There are ongoing discussions that

945 human embryo models should warrant careful regulations, and particularly those considered as
946 integrated ones should follow regulations similar to those for natural human embryos²¹⁸⁻²²⁰. Thus, we
947 need to be very cautious in choosing the most relevant embryo models for studies, while also
948 considering their ethical implications. It is desirable to choose ethically less challenging embryo models
949 if possible, when different models are available to recapitulate the developmental stages and associated
950 cell lineage developments of interest (**BOX 2**).

951 Appropriate embryo models need to be selected for specific applications. Increased cellular
952 complexity and composition in embryo models often come with decreased tissue organization and/or
953 model controllability and reproducibility. For example, studies of individual germ layer development
954 likely do not need the use of integrated embryo models that contain certain extraembryonic cell lineages.
955 In contrast, studies of tissue-tissue interactions, such as interactions between embryonic and
956 extraembryonic lineages, will require more complex embryo models that contain all relevant cell types⁸⁵⁻
957 ^{91,153,221}. For fundamental mechanistic studies to understand human development, embryo models that
958 closely resemble *in vivo* development in terms of lineage diversification, tissue patterning,
959 morphogenetic events, and tissue architecture will be desired. However, this might not be the case for
960 translational applications, especially high-content screening applications, which favor embryo models
961 with high reproducibility and scalability. For example, the 3D NT folding model faithfully recapitulates
962 the dynamic NP folding and provides a promising experimental tool to understand biomechanics of NT
963 closure¹⁴⁰. In contrast, 2D micropatterned neural rosette arrays, while they do not recapitulate the NP
964 folding morphogenesis, demonstrate high reproducibility, scalability and easy manipulation. As such,
965 2D micropatterned neural rosette arrays have already been successfully utilized for high-content screens
966 of factors that might disrupt neurulation and cause NTDs^{165,222,223}.

967 The field of stem cell-based embryo models is progressing rapidly, with tremendous potentials
968 for both fundamental and translational applications. Continuous development and broad applications of
969 embryo models will require the integrations of bioengineering approaches for improving cellular
970 complexity, composition and organization in embryo models and enhancing efficiency, controllability,
971 reproducibility, scalability and thus usefulness of the models. As this field moves forward, we should
972 keep in mind social responsibility as an essential part of the responsible conduct of research.
973 Transparency and effective engagement with all stakeholders including the public is essential to ensure
974 that promising avenues for research proceed with due caution, especially given the complexity and rapid
975 progress of this field.

976

977 **ACKNOWLEDGEMENTS**

978 The authors thank M. Yang for invaluable work on illustrations. Embryo modeling research in the Fu
979 laboratory is supported by the Michigan-Cambridge Collaboration Initiative, University of Michigan
980 Mcubed Fund, University of Michigan Mid-career Biosciences Faculty Achievement Recognition
981 Award, National Science Foundation (PFI-TT 2213845, I-Corps 2112458, CMMI 1917304, CBET
982 1901718, and CMMI 2325361) and National Institutes of Health (R21 NS113518, R21 HD100931, R21
983 HD105126, R21 NS127983, R21 HD109635, R21 HD105192, R33 CA261696, R01 GM134535 and
984 R01 NS129850). The authors apologize to all researchers whose work could not be cited owing to space
985 restrictions.

986

987 **AUTHOR CONTRIBUTIONS**

988 X.X., Y.L. and J.F. wrote article text. X.X. generated figures. All authors contributed to the
989 conceptualization of the article.

991 **COMPETING INTERESTS**

992 The authors declare no competing interests.

993

994

REFERENCES

996 1 Wolpert, L., Tickle, C. & Arias, A. M. *Principles of development*. (Oxford University Press, USA, 2015).
 997 2 Simunovic, M. & Brivanlou, A. H. Embryoids, organoids and gastruloids: New approaches to
 998 understanding embryogenesis. *Development* **144**, 976-985 (2017).
 999 3 Fu, J., Warmflash, A. & Lutolf, M. P. Stem-cell-based embryo models for fundamental research and
 1000 translation. *Nature Materials* **20**, 132-144 (2021).
 1001 4 Rossant, J. & Tam, P. P. L. Opportunities and Challenges with Stem Cell-Based Embryo Models. *Stem
 1002 Cell Reports* **16**, 1031-1038 (2021).
 1003 5 Shahbazi, M. N., Siggia, E. D. & Zernicka-Goetz, M. Self-organization of stem cells into embryos: A
 1004 window on early mammalian development. *Science* **364**, 948-951 (2019).
 1005 6 Keller, G. Embryonic stem cell differentiation: emergence of a new era in biology and medicine. *Genes
 1006 Dev* **19**, 1129-1155 (2005).
 1007 7 Sasai, Y. Cytosystems dynamics in self-organization of tissue architecture. *Nature* **493**, 318-326 (2013).
 1008 8 Turner, D. A., Baillie-Johnson, P. & Martinez Arias, A. Organoids and the genetically encoded self-
 1009 assembly of embryonic stem cells. *BioEssays* **38**, 181-191 (2016).
 1010 9 Terhune, A. H., Bok, J., Sun, S. & Fu, J. Stem cell-based models of early mammalian development.
 1011 *Development* **149** (2022).
 1012 10 Moris, N., Alev, C., Pera, M. & Martinez Arias, A. Biomedical and societal impacts of in vitro embryo
 1013 models of mammalian development. *Stem Cell Reports* **16**, 1021-1030 (2021).
 1014 11 Rossant, J. Why study human embryo development? *Dev Biol* **509**, 43-50 (2024).
 1015 12 Balázs, G., van Oudenaarden, A. & Collins, James J. Cellular Decision Making and Biological Noise:
 1016 From Microbes to Mammals. *Cell* **144**, 910-925 (2011).
 1017 13 Shao, Y. & Fu, J. Engineering multiscale structural orders for high-fidelity embryoids and organoids. *Cell
 1018 Stem Cell* **29**, 722-743 (2022).
 1019 14 Tanaka, S., Kunath, T., Hadjantonakis, A.-K., Nagy, A. & Rossant, J. Promotion of Trophoblast Stem
 1020 Cell Proliferation by FGF4. *Science* **282**, 2072-2075 (1998).
 1021 15 Okae, H. *et al.* Derivation of Human Trophoblast Stem Cells. *Cell Stem Cell* **22**, 50-63.e56 (2018).
 1022 16 Kunath, T. *et al.* Imprinted X-inactivation in extra-embryonic endoderm cell lines from mouse
 1023 blastocysts. (2005).
 1024 17 Du, P. & Wu, J. Hallmarks of totipotent and pluripotent stem cell states. *Cell Stem Cell* **31**, 312-333
 1025 (2024).
 1026 18 Salazar-Ciudad, I., Jernvall, J. & Newman, S. A. Mechanisms of pattern formation in development and
 1027 evolution. *Development* **130**, 2027-2037 (2003).
 1028 19 Schweisguth, F. & Corson, F. Self-Organization in Pattern Formation. *Developmental Cell* **49**, 659-677
 1029 (2019).
 1030 20 Simsek, M. F. & Özbudak, E. M. Patterning principles of morphogen gradients. *Open Biology* **12**, 220224
 1031 (2022).
 1032 21 Turing, A. M. The chemical basis of morphogenesis. *Bulletin of mathematical biology* **52**, 153-197
 1033 (1990).
 1034 22 Sick, S., Reinker, S., Timmer, J. & Schlake, T. WNT and DKK determine hair follicle spacing through a
 1035 reaction-diffusion mechanism. *Science* **314**, 1447-1450 (2006).
 1036 23 Etoc, F. *et al.* A Balance between Secreted Inhibitors and Edge Sensing Controls Gastruloid Self-
 1037 Organization. *Dev Cell* **39**, 302-315 (2016).
 1038 24 Kagawa, H. *et al.* Human blastoids model blastocyst development and implantation. *Nature* **601**, 600-605
 1039 (2022).
 1040 25 Warmflash, A., Sorre, B., Etoc, F., Siggia, E. D. & Brivanlou, A. H. A method to recapitulate early
 1041 embryonic spatial patterning in human embryonic stem cells. *Nature Methods* **11**, 847-854 (2014).
 1042 26 Wolpert, L. in *Current Topics in Developmental Biology* Vol. 117 (ed Paul M. Wassarman) 597-608
 1043 (Academic Press, 2016).

1044 27 Dessaud, E. *et al.* Interpretation of the sonic hedgehog morphogen gradient by a temporal adaptation
1045 mechanism. *Nature* **450**, 717-720 (2007).

1046 28 Heemskerk, I. *et al.* Rapid changes in morphogen concentration control self-organized patterning in
1047 human embryonic stem cells. *eLife* **8**, e40526 (2019).

1048 29 Tewary, M. *et al.* A stepwise model of reaction-diffusion and positional information governs self-
1049 organized human peri-gastrulation-like patterning. *Development* **144**, 4298-4312 (2017).

1050 30 Sun, S., Xue, X. & Fu, J. Modeling development using microfluidics: bridging gaps to foster fundamental
1051 and translational research. *Current Opinion in Genetics & Development* **82**, 102097 (2023).

1052 31 Xu, P.-F. *et al.* Construction of a mammalian embryo model from stem cells organized by a morphogen
1053 signalling centre. *Nature Communications* **12**, 3277 (2021).

1054 32 Zheng, Y. *et al.* Controlled modelling of human epiblast and amnion development using stem cells.
1055 *Nature* **573**, 421-425 (2019).

1056 33 Rifes, P. *et al.* Modeling neural tube development by differentiation of human embryonic stem cells in a
1057 microfluidic WNT gradient. *Nature Biotechnology* **38**, 1265-1273 (2020).

1058 34 Xue, X. *et al.* A patterned human neural tube model using microfluidic gradients. *Nature* (2024).

1059 35 Morales, J. S., Raspopovic, J. & Marcon, L. From embryos to embryoids: How external signals and self-
1060 organization drive embryonic development. *Stem Cell Reports* **16**, 1039-1050 (2021).

1061 36 Rossant, J. & Tam, P. P. L. Blastocyst lineage formation, early embryonic asymmetries and axis
1062 patterning in the mouse. *Development* **136**, 701-713 (2009).

1063 37 Wennekamp, S., Mesecke, S., Nédélec, F. & Hiragi, T. A self-organization framework for symmetry
1064 breaking in the mammalian embryo. *Nature Reviews Molecular Cell Biology* **14**, 452-459 (2013).

1065 38 Maître, J.-L., Niwayama, R., Turlier, H., Nédélec, F. & Hiragi, T. Pulsatile cell-autonomous contractility
1066 drives compaction in the mouse embryo. *Nature Cell Biology* **17**, 849-855 (2015).

1067 39 Fleming, T. P., Cannon, P. M. & Pickering, S. J. The cytoskeleton, endocytosis and cell polarity in the
1068 mouse preimplantation embryo. *Developmental biology* **113**, 406-419 (1986).

1069 40 Wicklow, E. *et al.* HIPPO pathway members restrict SOX2 to the inner cell mass where it promotes ICM
1070 fates in the mouse blastocyst. *PLoS genetics* **10**, e1004618 (2014).

1071 41 Nishioka, N. *et al.* The Hippo signaling pathway components Lats and Yap pattern Tead4 activity to
1072 distinguish mouse trophectoderm from inner cell mass. *Developmental cell* **16**, 398-410 (2009).

1073 42 Maître, J.-L. *et al.* Asymmetric division of contractile domains couples cell positioning and fate
1074 specification. *Nature* **536**, 344-348 (2016).

1075 43 Korotkevich, E. *et al.* The Apical Domain Is Required and Sufficient for the First Lineage Segregation in
1076 the Mouse Embryo. *Developmental Cell* **40**, 235-247.e237 (2017).

1077 44 Niwayama, R. *et al.* A Tug-of-War between Cell Shape and Polarity Controls Division Orientation to
1078 Ensure Robust Patterning in the Mouse Blastocyst. *Dev Cell* **51**, 564-574.e566 (2019).

1079 45 Barcroft, L. C., Offenberg, H., Thomsen, P. & Watson, A. J. Aquaporin proteins in murine trophectoderm
1080 mediate transepithelial water movements during cavitation. *Developmental biology* **256**, 342-354 (2003).

1081 46 Dumortier, J. G. *et al.* Hydraulic fracturing and active coarsening position the lumen of the mouse
1082 blastocyst. *Science* **365**, 465-468 (2019).

1083 47 Kang, M., Garg, V. & Hadjantonakis, A.-K. Lineage establishment and progression within the inner cell
1084 mass of the mouse blastocyst requires FGFR1 and FGFR2. *Developmental cell* **41**, 496-510. e495 (2017).

1085 48 Saiz, N., Grabarek, J. B., Sabherwal, N., Papalopulu, N. & Plusa, B. Atypical protein kinase C couples
1086 cell sorting with primitive endoderm maturation in the mouse blastocyst. *Development* **140**, 4311-4322
1087 (2013).

1088 49 Kuijk, E. W. *et al.* The roles of FGF and MAP kinase signaling in the segregation of the epiblast and
1089 hypoblast cell lineages in bovine and human embryos. *Development* **139**, 871-882 (2012).

1090 50 Roode, M. *et al.* Human hypoblast formation is not dependent on FGF signalling. *Developmental biology*
1091 **361**, 358-363 (2012).

1092 51 Dattani, A. *et al.* Human naïve stem cell models reveal the role of FGF in hypoblast specification in the
1093 human embryo. *bioRxiv*, 2023.2011.2030.569161 (2023).

1094 52 Linneberg-Agerholm, M. *et al.* Naïve human pluripotent stem cells respond to Wnt, Nodal and LIF
1095 signalling to produce expandable naïve extra-embryonic endoderm. *Development* **146** (2019).

1096 53 Rivron, N. C. *et al.* Blastocyst-like structures generated solely from stem cells. *Nature* **557**, 106-111
1097 (2018).

1098 54 Sozen, B. *et al.* Self-Organization of Mouse Stem Cells into an Extended Potential Blastoid.
1099 *Developmental Cell* **51**, 698-712.e698 (2019).

1100 55 Li, R. *et al.* Generation of Blastocyst-like Structures from Mouse Embryonic and Adult Cell Cultures.
1101 *Cell* **179**, 687-702.e618 (2019).

1102 56 Liu, X. *et al.* Modelling human blastocysts by reprogramming fibroblasts into iBlastoids. *Nature* **591**,
1103 627-632 (2021).

1104 57 Yanagida, A. *et al.* Naive stem cell blastocyst model captures human embryo lineage segregation. *Cell
1105 Stem Cell* **28**, 1016-1022.e1014 (2021).

1106 58 Yu, L. *et al.* Blastocyst-like structures generated from human pluripotent stem cells. *Nature* **591**, 620-626
1107 (2021).

1108 59 Yu, L. *et al.* Large-scale production of human blastoids amenable to modeling blastocyst development
1109 and maternal-fetal cross talk. *Cell Stem Cell* **30**, 1246-1261.e1249 (2023).

1110 60 Sozen, B. *et al.* Reconstructing aspects of human embryogenesis with pluripotent stem cells. *Nature
1111 Communications* **12**, 5550 (2021).

1112 61 Guo, G. *et al.* Human naive epiblast cells possess unrestricted lineage potential. *Cell Stem Cell* **28**, 1040-
1113 1056.e1046 (2021).

1114 62 Shibata, S. *et al.* Modeling embryo-endometrial interface recapitulating human embryo implantation.
1115 *Science Advances* **10**, eadi4819 (2024).

1116 63 Rodriguez, T. A., Srinivas, S., Clements, M. P., Smith, J. C. & Beddington, R. S. P. Induction and
1117 migration of the anterior visceral endoderm is regulated by the extra-embryonic ectoderm. *Development*
1118 **132**, 2513-2520 (2005).

1119 64 Yamamoto, M. *et al.* Antagonism between Smad1 and Smad2 signaling determines the site of distal
1120 visceral endoderm formation in the mouse embryo. *Journal of Cell Biology* **184**, 323-334 (2009).

1121 65 Yamamoto, M. *et al.* Nodal antagonists regulate formation of the anteroposterior axis of the mouse
1122 embryo. *Nature* **428**, 387-392 (2004).

1123 66 Belo, J. A. *et al.* Cerberus-like is a secreted factor with neuralizing activity expressed in the anterior
1124 primitive endoderm of the mouse gastrula. *Mechanisms of development* **68**, 45-57 (1997).

1125 67 Kemp, C. R. *et al.* Expression of Frizzled5, Frizzled7, and Frizzled10 during early mouse development
1126 and interactions with canonical Wnt signaling. *Developmental Dynamics* **236**, 2011-2019 (2007).

1127 68 Rossant, J. & Tam, P. P. L. Early human embryonic development: Blastocyst formation to gastrulation.
1128 *Developmental Cell* **57**, 152-165 (2022).

1129 69 Molè, M. A. *et al.* A single cell characterisation of human embryogenesis identifies pluripotency
1130 transitions and putative anterior hypoblast centre. *Nature Communications* **12**, 3679 (2021).

1131 70 Zhu, Q. *et al.* Decoding anterior-posterior axis emergence among mouse, monkey, and human embryos.
1132 *Developmental Cell* **58**, 63-79.e64 (2023).

1133 71 Harrison, S. E., Sozen, B., Christodoulou, N., Kyprianou, C. & Zernicka-Goetz, M. Assembly of
1134 embryonic and extraembryonic stem cells to mimic embryogenesis in vitro. *Science* **356**, eaal1810 (2017).

1135 72 Sozen, B. *et al.* Self-assembly of embryonic and two extra-embryonic stem cell types into gastrulating
1136 embryo-like structures. *Nature Cell Biology* **20**, 979-989 (2018).

1137 73 Zhang, S. *et al.* Implantation initiation of self-assembled embryo-like structures generated using three
1138 types of mouse blastocyst-derived stem cells. *Nature Communications* **10**, 496 (2019).

1139 74 Aguilera-Castrejon, A. *et al.* Ex utero mouse embryogenesis from pre-gastrulation to late organogenesis.
1140 *Nature* **593**, 119-124 (2021).

1141 75 Amadei, G. *et al.* Embryo model completes gastrulation to neurulation and organogenesis. *Nature* **610**,
1142 143-153 (2022).

1143 76 Tarazi, S. *et al.* Post-gastrulation synthetic embryos generated ex utero from mouse naive ESCs. *Cell* **185**,
1144 3290-3306.e3225 (2022).

1145 77 Lau, K. Y. C. *et al.* Mouse embryo model derived exclusively from embryonic stem cells undergoes
1146 neurulation and heart development. *Cell Stem Cell* **29**, 1445-1458.e1448 (2022).

1147 78 Girgin, M. U. *et al.* Bioengineered embryoids mimic post-implantation development in vitro. *Nature
1148 Communications* **12**, 5140 (2021).

1149 79 Birey, F. *et al.* Assembly of functionally integrated human forebrain spheroids. *Nature* **545**, 54-59 (2017).

1150 80 Koike, H. *et al.* Modelling human hepato-biliary-pancreatic organogenesis from the foregut-midgut
1151 boundary. *Nature* **574**, 112-116 (2019).

1152 81 Simunovic, M. *et al.* A 3D model of a human epiblast reveals BMP4-driven symmetry breaking. *Nature
1153 Cell Biology* **21**, 900-910 (2019).

1154 82 Simunovic, M., Siggia, E. D. & Brivanlou, A. H. In vitro attachment and symmetry breaking of a human
1155 embryo model assembled from primed embryonic stem cells. *Cell Stem Cell* **29**, 962-972.e964 (2022).

1156 83 Shao, Y. *et al.* A pluripotent stem cell-based model for post-implantation human amniotic sac
1157 development. *Nature Communications* **8**, 208 (2017).

1158 84 Yang, R. *et al.* Amnion signals are essential for mesoderm formation in primates. *Nature
1159 Communications* **12**, 5126 (2021).

1160 85 Karvas, R. M. *et al.* 3D-cultured blastoids model human embryogenesis from pre-implantation to early
1161 gastrulation stages. *Cell Stem Cell* **30**, 1148-1165.e1147 (2023).

1162 86 Hislop, J. *et al.* Modelling post-implantation human development to yolk sac blood emergence. *Nature
1163* (2023).

1164 87 Liu, L. *et al.* Modeling post-implantation stages of human development into early organogenesis with
1165 stem-cell-derived peri-gastruloids. *Cell* (2023).

1166 88 Oldak, B. *et al.* Complete human day 14 post-implantation embryo models from naive ES cells. *Nature
1167* **622**, 562-573 (2023).

1168 89 Pedroza, M. *et al.* Self-patterning of human stem cells into post-implantation lineages. *Nature* (2023).

1169 90 Weatherbee, B. A. T. *et al.* Pluripotent stem cell-derived model of the post-implantation human embryo.
1170 *Nature* **622**, 584-593 (2023).

1171 91 Okubo, T. *et al.* Hypoblast from human pluripotent stem cells regulates epiblast development. *Nature
1172* **626**, 357-366 (2024).

1173 92 Storey, K. G. *et al.* Early posterior neural tissue is induced by FGF in the chick embryo. *Development
1174* **125**, 473-484 (1998).

1175 93 Niederreither, K., Subbarayan, V., Dollé, P. & Chambon, P. Embryonic retinoic acid synthesis is essential
1176 for early mouse post-implantation development. *Nature Genetics* **21**, 444-448 (1999).

1177 94 Nordström, U., Jessell, T. M. & Edlund, T. Progressive induction of caudal neural character by graded
1178 Wnt signaling. *Nature Neuroscience* **5**, 525-532 (2002).

1179 95 Wurst, W. & Bally-Cuif, L. Neural plate patterning: Upstream and downstream of the isthmic organizer.
1180 *Nature Reviews Neuroscience* **2**, 99-108 (2001).

1181 96 Sagner, A. & Briscoe, J. Establishing neuronal diversity in the spinal cord: a time and a place.
1182 *Development* **146** (2019).

1183 97 Wilson, S. W. & Rubenstein, J. L. R. Induction and Dorsoventral Patterning of the Telencephalon.
1184 *Neuron* **28**, 641-651 (2000).

1185 98 Wilson, L., Gale, E., Chambers, D. & Maden, M. Retinoic acid and the control of dorsoventral patterning
1186 in the avian spinal cord. *Developmental Biology* **269**, 433-446 (2004).

1187 99 Meinhardt, A. *et al.* 3D reconstitution of the patterned neural tube from embryonic stem cells. *Stem Cell
1188 Reports* **3**, 987-999 (2014).

1189 100 Zheng, Y. *et al.* Dorsal-ventral patterned neural cyst from human pluripotent stem cells in a neurogenic
1190 niche. *Science Advances* **5**, eaax5933 (2019).

1191 101 Ranga, A. *et al.* Neural tube morphogenesis in synthetic 3D microenvironments. *Proceedings of the
1192 National Academy of Sciences* **113**, E6831-E6839 (2016).

1193 102 Abdel Fattah, A. R., Grebenyuk, S., de Rooij, L. P. M. H., Salmon, I. & Ranga, A. Neuroepithelial
1194 organoid patterning is mediated by a neighborhood watch mechanism. *Cell Reports* **42**, 113334 (2023).

1195 103 Krammer, T. *et al.* Neural tube organoids self-organise floorplate through BMP-mediated cluster
1196 104 competition. *bioRxiv*, 2023.2006.2025.546258 (2023).

1197 104 Pavon, N. *et al.* Patterning ganglionic eminences in developing human brain organoids using a
1198 105 morphogen-gradient-inducing device. *Cell Rep Methods* **4**, 100689 (2024).

1199 105 Gjorevski, N. *et al.* Tissue geometry drives deterministic organoid patterning. *Science* **375**, eaaw9021
1200 106 (2022).

1201 106 Nikolaev, M. *et al.* Homeostatic mini-intestines through scaffold-guided organoid morphogenesis. *Nature*
1202 107 **585**, 574-578 (2020).

1203 107 Rodriguez, N. M., Desai, R. A., Trappmann, B., Baker, B. M. & Chen, C. S. Micropatterned Multicolor
1204 108 Dynamically Adhesive Substrates to Control Cell Adhesion and Multicellular Organization. *Langmuir* **30**,
1205 1327-1335 (2014).

1206 108 Wright, D., Rajalingam, B., Selvarasah, S., Dokmeci, M. R. & Khademhosseini, A. Generation of static
1207 109 and dynamic patterned co-cultures using microfabricated parylene-C stencils. *Lab on a Chip* **7**, 1272-
1208 1279 (2007).

1209 109 March, S. *et al.* Micropatterned coculture of primary human hepatocytes and supportive cells for the study
1210 110 of hepatotropic pathogens. *Nature Protocols* **10**, 2027-2053 (2015).

1211 110 Li, C. Y. *et al.* Micropatterned cell-cell interactions enable functional encapsulation of primary
1212 111 hepatocytes in hydrogel microtissues. *Tissue Eng Part A* **20**, 2200-2212 (2014).

1213 111 Hui, E. E. & Bhatia, S. N. Micromechanical control of cell-cell interactions. *Proceedings of the National
1214 112 Academy of Sciences* **104**, 5722-5726 (2007).

1215 112 Manfrin, A. *et al.* Engineered signaling centers for the spatially controlled patterning of human
1216 113 pluripotent stem cells. *Nature Methods* **16**, 640-648 (2019).

1217 113 Xue, X. *et al.* Mechanics-guided embryonic patterning of neuroectoderm tissue from human pluripotent
1218 114 stem cells. *Nature Materials* **17**, 633-641 (2018).

1219 114 Khadir, Z. *et al.* Surface micropatterning for the formation of an in vitro functional endothelial model for
1220 115 cell-based biosensors. *Biosensors and Bioelectronics* **214**, 114481 (2022).

1221 115 Murphy, S. V. & Atala, A. 3D bioprinting of tissues and organs. *Nature Biotechnology* **32**, 773-785
1222 116 (2014).

1223 116 Banerjee, D. *et al.* Strategies for 3D bioprinting of spheroids: A comprehensive review. *Biomaterials* **291**,
1224 121881 (2022).

1225 117 Daly, A. C., Davidson, M. D. & Burdick, J. A. 3D bioprinting of high cell-density heterogeneous tissue
1226 118 models through spheroid fusion within self-healing hydrogels. *Nature Communications* **12**, 753 (2021).

1227 118 Roth, J. G. *et al.* Spatially controlled construction of assembloids using bioprinting. *Nature
1228 119 Communications* **14**, 4346 (2023).

1229 119 Skylar-Scott, M. A. *et al.* Biomanufacturing of organ-specific tissues with high cellular density and
1230 120 embedded vascular channels. *Science Advances* **5**, eaaw2459 (2019).

1231 120 Ben-Reuven, L. & Reiner, O. Toward Spatial Identities in Human Brain Organoids-on-Chip Induced by
1232 121 Morphogen-Soaked Beads. *Bioengineering* **7**, 164 (2020).

1233 121 Marín-Llera, J. C. & Chimal-Monroy, J. Analysis of Cell Differentiation, Morphogenesis, and Patterning
1234 122 During Chicken Embryogenesis Using the Soaked-Bead Assay. *J Vis Exp* (2022).

1235 122 Bonner, M. G., Gudapati, H., Mou, X. & Musah, S. Microfluidic systems for modeling human
1236 123 development. *Development* **149** (2022).

1237 123 Sonnen, K. F. & Merten, C. A. Microfluidics as an emerging precision tool in developmental biology.
1238 124 *Developmental cell* **48**, 293-311 (2019).

1239 124 Cederquist, G. Y. *et al.* Specification of positional identity in forebrain organoids. *Nat Biotechnol* **37**,
1240 125 436-444 (2019).

1241 125 Toda, S. *et al.* Engineering synthetic morphogen systems that can program multicellular patterning.
1242 126 *Science* **370**, 327-331 (2020).

1243 126 Legnini, I. *et al.* Spatiotemporal, optogenetic control of gene expression in organoids. *Nature Methods* **20**,
1244 1544-1552 (2023).

1245 127 Martínez-Ara, G. *et al.* Optogenetic control of apical constriction induces synthetic morphogenesis in
1246 mammalian tissues. *Nature Communications* **13**, 5400 (2022).

1247 128 Gurdon, J. B., Harger, P., Mitchell, A. & Lemaire, P. Activin signalling and response to a morphogen
1248 gradient. *Nature* **371**, 487-492 (1994).

1249 129 Gurdon, J., Mitchell, A. & Mahony, D. Direct and continuous assessment by cells of their position in a
1250 morphogen gradient. *Nature* **376**, 520-521 (1995).

1251 130 Reyes, D. R. *et al.* Accelerating innovation and commercialization through standardization of
1252 microfluidic-based medical devices. *Lab on a Chip* **21**, 9-21 (2021).

1253 131 Repina, N. A. *et al.* Optogenetic control of Wnt signaling models cell-intrinsic embryogenic patterning
1254 using 2D human pluripotent stem cell culture. *Development* **150** (2023).

1255 132 De Santis, R., Etoc, F., Rosado-Olivieri, E. A. & Brivanlou, A. H. Self-organization of human dorsal-
1256 ventral forebrain structures by light induced SHH. *Nature Communications* **12**, 6768 (2021).

1257 133 Emiliani, V. *et al.* Optogenetics for light control of biological systems. *Nat Rev Methods Primers* **2**
1258 (2022).

1259 134 Sheng, G., Martinez Arias, A. & Sutherland, A. The primitive streak and cellular principles of building an
1260 amniote body through gastrulation. *Science* **374**, abg1727 (2021).

1261 135 Miao, Y. & Pourquié, O. Cellular and molecular control of vertebrate somitogenesis. *Nature Reviews
1262 Molecular Cell Biology* (2024).

1263 136 Nikolopoulou, E., Galea, G. L., Rolo, A., Greene, N. D. E. & Copp, A. J. Neural tube closure: cellular,
1264 molecular and biomechanical mechanisms. *Development* **144**, 552-566 (2017).

1265 137 Walma, D. A. C. & Yamada, K. M. The extracellular matrix in development. *Development* **147** (2020).

1266 138 Kratochvil, M. J. *et al.* Engineered materials for organoid systems. *Nature Reviews Materials* **4**, 606-622
1267 (2019).

1268 139 van den Brink, S. C. *et al.* Single-cell and spatial transcriptomics reveal somitogenesis in gastruloids.
1269 *Nature* **582**, 405-409 (2020).

1270 140 Karzbrun, E. *et al.* Human neural tube morphogenesis in vitro by geometric constraints. *Nature* **599**, 268-
1271 272 (2021).

1272 141 Veenvliet, J. V. *et al.* Mouse embryonic stem cells self-organize into trunk-like structures with neural
1273 tube and somites. *Science* **370**, eaba4937 (2020).

1274 142 Steventon, B., Busby, L. & Arias, A. M. Establishment of the vertebrate body plan: Rethinking
1275 gastrulation through stem cell models of early embryogenesis. *Developmental Cell* **56**, 2405-2418 (2021).

1276 143 Zhang, Z., Zwick, S., Loew, E., Grimley, J. S. & Ramanathan, S. Mouse embryo geometry drives
1277 formation of robust signaling gradients through receptor localization. *Nature Communications* **10**, 4516
1278 (2019).

1279 144 Beccari, L. *et al.* Multi-axial self-organization properties of mouse embryonic stem cells into gastruloids.
1280 *Nature* **562**, 272-276 (2018).

1281 145 Moris, N. *et al.* An in vitro model of early anteroposterior organization during human development.
1282 *Nature* **582**, 410-415 (2020).

1283 146 Sullivan, A. E. & Santos, S. D. M. The ever-growing world of gastruloids: autogenous models of
1284 mammalian embryogenesis. *Current Opinion in Genetics & Development* **82**, 102102 (2023).

1285 147 Rossi, G. *et al.* Capturing Cardiogenesis in Gastruloids. *Cell Stem Cell* **28**, 230-240.e236 (2021).

1286 148 Vianello, S. & Lutolf, M. P. *In vitro* endoderm emergence and self-organisation in the
1287 absence of extraembryonic tissues and embryonic architecture. *bioRxiv*, 2020.2006.2007.138883 (2021).

1288 149 Sozen, B., Conkar, D. & Veenvliet, J. V. Carnegie in 4D? Stem-cell-based models of human embryo
1289 development. *Seminars in Cell & Developmental Biology* **131**, 44-57 (2022).

1290 150 Muncie, J. M. *et al.* Mechanical Tension Promotes Formation of Gastrulation-like Nodes and Patterns
1291 Mesoderm Specification in Human Embryonic Stem Cells. *Developmental Cell* **55**, 679-694.e611 (2020).

1292 151 Caldarelli, P., Chamolly, A., Alegria-Prévet, O., Gros, J. & Corson, F. Self-organized tissue mechanics
1293 underlie embryonic regulation. *bioRxiv*, 2021.2010.2008.463661 (2021).

1294 152 Brunet, T. *et al.* Evolutionary conservation of early mesoderm specification by mechanotransduction in
1295 Bilateria. *Nat Commun* **4**, 2821 (2013).

1296 153 Liu, L. *et al.* Modeling post-implantation stages of human development into early organogenesis with
1297 stem-cell-derived peri-gastruloids. *Cell* **186**, 3776-3792.e3716 (2023).

1298 154 Tzouanacou, E., Wegener, A., Wymeersch, F. J., Wilson, V. & Nicolas, J.-F. Redefining the Progression
1299 of Lineage Segregations during Mammalian Embryogenesis by Clonal Analysis. *Developmental Cell* **17**,
1300 365-376 (2009).

1301 155 Underhill, E. J. & Toettcher, J. E. Control of gastruloid patterning and morphogenesis by the Erk and Akt
1302 signaling pathways. *Development* **150** (2023).

1303 156 de Jong, M. A. *et al.* The shapes of elongating gastruloids are consistent with convergent extension driven
1304 by a combination of active cell crawling and differential adhesion. *PLOS Computational Biology* **20**,
1305 e1011825 (2024).

1306 157 Sutherland, A., Keller, R. & Lesko, A. Convergent extension in mammalian morphogenesis. *Semin Cell*
1307 *Dev Biol* **100**, 199-211 (2020).

1308 158 Moon, L. D. & Xiong, F. Mechanics of neural tube morphogenesis. *Seminars in Cell & Developmental*
1309 *Biology* **130**, 56-69 (2022).

1310 159 van der Spuy, M., Wang, J. X., Kociszewska, D. & White, M. D. The cellular dynamics of neural tube
1311 formation. *Biochemical Society Transactions* **51**, 343-352 (2023).

1312 160 Nakatsu, T., Uwabe, C. & Shiota, K. Neural tube closure in humans initiates at multiple sites: evidence
1313 from human embryos and implications for the pathogenesis of neural tube defects. *Anatomy and*
1314 *embryology* **201**, 455-466 (2000).

1315 161 Greene, N. D. E. & Copp, A. J. Neural Tube Defects. *Annual Review of Neuroscience* **37**, 221-242
1316 (2014).

1317 162 Morris-Kay, G. & Tuckett, F. The role of microfilaments in cranial neurulation in rat embryos: effects of
1318 short-term exposure to cytochalasin D. *Development* **88**, 333-348 (1985).

1319 163 Ybot-Gonzalez, P. & Copp, A. J. Bending of the neural plate during mouse spinal neurulation is
1320 independent of actin microfilaments. *Developmental Dynamics* **215**, 273-283 (1999).

1321 164 Gurniak, C. B., Perlas, E. & Witke, W. The actin depolymerizing factor n-cofilin is essential for neural
1322 tube morphogenesis and neural crest cell migration. *Developmental biology* **278**, 231-241 (2005).

1323 165 Knight, G. T. *et al.* Engineering induction of singular neural rosette emergence within hPSC-derived
1324 tissues. *eLife* **7**, e37549 (2018).

1325 166 Britton, G., Heemskerk, I., Hodge, R., Qutub, A. A. & Warmflash, A. A novel self-organizing embryonic
1326 stem cell system reveals signaling logic underlying the patterning of human ectoderm. *Development* **146**
1327 (2019).

1328 167 Haremaiki, T. *et al.* Self-organizing neuruloids model developmental aspects of Huntington's disease in
1329 the ectodermal compartment. *Nature Biotechnology* **37**, 1198-1208 (2019).

1330 168 Lee, J.-H. *et al.* Production of human spinal-cord organoids recapitulating neural-tube morphogenesis.
1331 *Nature Biomedical Engineering* **6**, 435-448 (2022).

1332 169 Fedorova, V. *et al.* Differentiation of neural rosettes from human pluripotent stem cells in vitro is
1333 sequentially regulated on a molecular level and accomplished by the mechanism reminiscent of secondary
1334 neurulation. *Stem Cell Research* **40**, 101563 (2019).

1335 170 Kulesa, P. M. & Fraser, S. E. Cell Dynamics During Somite Boundary Formation Revealed by Time-
1336 Lapse Analysis. *Science* **298**, 991-995 (2002).

1337 171 Sato, Y. & Takahashi, Y. A novel signal induces a segmentation fissure by acting in a ventral-to-dorsal
1338 direction in the presomitic mesoderm. *Developmental Biology* **282**, 183-191 (2005).

1339 172 Marrese, M. *et al.* In vivo characterization of chick embryo mesoderm by optical coherence tomography-
1340 assisted microindentation. *Faseb j* **34**, 12269-12277 (2020).

1341 173 Nelemans, B. K. A., Schmitz, M., Tahir, H., Merks, R. M. H. & Smit, T. H. Somite Division and New
1342 Boundary Formation by Mechanical Strain. *iScience* **23**, 100976 (2020).

1343 174 Adhyapok, P. *et al.* A mechanical model of early somite segmentation. *iScience* **24**, 102317 (2021).

1344 175 Sanaki-Matsumiya, M. *et al.* Periodic formation of epithelial somites from human pluripotent stem cells.
1345 *Nature Communications* **13**, 2325 (2022).

1346 176 Yaman, Y. I. & Ramanathan, S. Controlling human organoid symmetry breaking reveals signaling
1347 gradients drive segmentation clock waves. *Cell* **186**, 513-527.e519 (2023).

1348 177 Miao, Y. *et al.* Reconstruction and deconstruction of human somitogenesis in vitro. *Nature* **614**, 500-508
1349 (2023).

1350 178 Yamanaka, Y. *et al.* Reconstituting human somitogenesis in vitro. *Nature* **614**, 509-520 (2023).

1351 179 Liu, Y. *et al.* A human pluripotent stem cell-based somitogenesis model using microfluidics. *bioRxiv*,
1352 2023.2010.2029.564399 (2023).

1353 180 Gribaldo, S. *et al.* Self-organizing models of human trunk organogenesis recapitulate spinal cord and
1354 spine co-morphogenesis. *Nature Biotechnology* (2023).

1355 181 Alom Ruiz, S. & Chen, C. S. Microcontact printing: A tool to pattern. *Soft Matter* **3**, 168-177 (2007).

1356 182 Sahni, G., Yuan, J. & Toh, Y. C. Stencil Micropatterning of Human Pluripotent Stem Cells for Probing
1357 Spatial Organization of Differentiation Fates. *J Vis Exp* (2016).

1358 183 Folch, A., Jo, B.-H., Hurtado, O., Beebe, D. J. & Toner, M. Microfabricated elastomeric stencils for
1359 micropatterning cell cultures. *Journal of Biomedical Materials Research* **52**, 346-353 (2000).

1360 184 Kay, R. & Desmulliez, M. A review of stencil printing for microelectronic packaging. *Soldering &*
1361 *Surface Mount Technology* **24**, 38-50 (2012).

1362 185 Du, K., Ding, J., Liu, Y., Wathuthantri, I. & Choi, C.-H. Stencil Lithography for Scalable Micro- and
1363 Nanomanufacturing. *Micromachines* **8**, 131 (2017).

1364 186 Dillmore, W. S., Yousaf, M. N. & Mrksich, M. A Photochemical Method for Patterning the
1365 Immobilization of Ligands and Cells to Self-Assembled Monolayers. *Langmuir* **20**, 7223-7231 (2004).

1366 187 Peterbauer, T., Heitz, J., Olbrich, M. & Hering, S. Simple and versatile methods for the fabrication of
1367 arrays of live mammalian cells. *Lab on a Chip* **6**, 857-863 (2006).

1368 188 Gumpenberger, T. *et al.* Adhesion and proliferation of human endothelial cells on photochemically
1369 modified polytetrafluoroethylene. *Biomaterials* **24**, 5139-5144 (2003).

1370 189 Aisenbrey, E. A. & Murphy, W. L. Synthetic alternatives to Matrigel. *Nature Reviews Materials* **5**, 539-
1371 551 (2020).

1372 190 Gjorevski, N. *et al.* Designer matrices for intestinal stem cell and organoid culture. *Nature* **539**, 560-564
1373 (2016).

1374 191 Cruz-Acuña, R. *et al.* Synthetic hydrogels for human intestinal organoid generation and colonic wound
1375 repair. *Nature Cell Biology* **19**, 1326-1335 (2017).

1376 192 Enemchukwu, N. O. *et al.* Synthetic matrices reveal contributions of ECM biophysical and biochemical
1377 properties to epithelial morphogenesis. *Journal of Cell Biology* **212**, 113-124 (2015).

1378 193 Blatchley, M. R. & Anseth, K. S. Middle-out methods for spatiotemporal tissue engineering of organoids.
1379 *Nature Reviews Bioengineering* **1**, 329-345 (2023).

1380 194 DeForest, C. A. & Tirrell, D. A. A photoreversible protein-patterning approach for guiding stem cell fate
1381 in three-dimensional gels. *Nature Materials* **14**, 523-531 (2015).

1382 195 Grim, J. C. *et al.* A Reversible and Repeatable Thiol-Ene Bioconjugation for Dynamic Patterning of
1383 Signaling Proteins in Hydrogels. *ACS Central Science* **4**, 909-916 (2018).

1384 196 Jeon, O., Lee, K. & Alsberg, E. Spatial Micropatterning of Growth Factors in 3D Hydrogels for Location-
1385 Specific Regulation of Cellular Behaviors. *Small* **14**, 1800579 (2018).

1386 197 Pedron, S. *et al.* Patterning three-dimensional hydrogel microenvironments using hyperbranched
1387 polyglycerols for independent control of mesh size and stiffness. *Biomacromolecules* **18**, 1393-1400
1388 (2017).

1389 198 Lee, S.-H., Moon, J. J. & West, J. L. Three-dimensional micropatterning of bioactive hydrogels via two-
1390 photon laser scanning photolithography for guided 3D cell migration. *Biomaterials* **29**, 2962-2968 (2008).

1391 199 Yavitt, F. M. *et al.* In situ modulation of intestinal organoid epithelial curvature through photoinduced
1392 viscoelasticity directs crypt morphogenesis. *Science Advances* **9**, eadd5668 (2023).

1393 200 Manhas, J., Edelstein, H. I., Leonard, J. N. & Morsut, L. The evolution of synthetic receptor systems.
1394 *Nature Chemical Biology* **18**, 244-255 (2022).

1395 201 Chen, W. C. W. *et al.* A synthetic transcription platform for programmable gene expression in
1396 mammalian cells. *Nature Communications* **13**, 6167 (2022).

1397 202 Toda, S., Blauch, L. R., Tang, S. K. Y., Morsut, L. & Lim, W. A. Programming self-organizing
1398 multicellular structures with synthetic cell-cell signaling. *Science* **361**, 156-162 (2018).

1399 203 Jurkowski, T. P., Ravichandran, M. & Stepper, P. Synthetic epigenetics—towards intelligent control of
1400 epigenetic states and cell identity. *Clinical Epigenetics* **7**, 18 (2015).

1401 204 Amadei, G. *et al.* Inducible Stem-Cell-Derived Embryos Capture Mouse Morphogenetic Events In Vitro.
1402 *Dev Cell* **56**, 366-382.e369 (2021).

1403 205 Skylar-Scott, M. A. *et al.* Orthogonally induced differentiation of stem cells for the programmatic
1404 patterning of vascularized organoids and bioprinted tissues. *Nature Biomedical Engineering* **6**, 449-462
1405 (2022).

1406 206 Duguay, D., Foty, R. A. & Steinberg, M. S. Cadherin-mediated cell adhesion and tissue segregation:
1407 qualitative and quantitative determinants. *Developmental Biology* **253**, 309-323 (2003).

1408 207 Foty, R. A. & Steinberg, M. S. The differential adhesion hypothesis: a direct evaluation. *Developmental
1409 Biology* **278**, 255-263 (2005).

1410 208 Bao, M. *et al.* Stem cell-derived synthetic embryos self-assemble by exploiting cadherin codes and
1411 cortical tension. *Nature Cell Biology* **24**, 1341-1349 (2022).

1412 209 Stevens, A. J. *et al.* Programming multicellular assembly with synthetic cell adhesion molecules. *Nature
1413* **614**, 144-152 (2023).

1414 210 Deglincerti, A. *et al.* Self-organization of the in vitro attached human embryo. *Nature* **533**, 251-254
1415 (2016).

1416 211 Shahbazi, M. N. *et al.* Self-organization of the human embryo in the absence of maternal tissues. *Nature
1417 Cell Biology* **18**, 700-708 (2016).

1418 212 Zhai, J. *et al.* Primate gastrulation and early organogenesis at single-cell resolution. *Nature* **612**, 732-738
1419 (2022).

1420 213 Gong, Y. *et al.* Ex utero monkey embryogenesis from blastocyst to early organogenesis. *Cell* **186**, 2092-
1421 2110.e2023 (2023).

1422 214 Xu, Y. *et al.* A single-cell transcriptome atlas profiles early organogenesis in human embryos. *Nature
1423 Cell Biology* **25**, 604-615 (2023).

1424 215 Tyser, R. C. V. *et al.* Single-cell transcriptomic characterization of a gastrulating human embryo. *Nature
1425* **600**, 285-289 (2021).

1426 216 Zeng, B. *et al.* The single-cell and spatial transcriptional landscape of human gastrulation and early brain
1427 development. *Cell Stem Cell* **30**, 851-866.e857 (2023).

1428 217 Meistermann, D. *et al.* Integrated pseudotime analysis of human pre-implantation embryo single-cell
1429 transcriptomes reveals the dynamics of lineage specification. *Cell Stem Cell* **28**, 1625-1640. e1626
1430 (2021).

1431 218 Rossant, J. & Fu, J. Why researchers should use human embryo models with caution. *Nature* (2023).

1432 219 Rivron, N. C., Martinez Arias, A., Pera, M. F., Moris, N. & M'hamdi, H. I. An ethical framework for
1433 human embryology with embryo models. *Cell* **186**, 3548-3557 (2023).

1434 220 Clark, A. T. *et al.* Human embryo research, stem cell-derived embryo models and in vitro gametogenesis:
1435 Considerations leading to the revised ISSCR guidelines. *Stem Cell Rep.* **16**, 1416-1424 (2021).

1436 221 Oldak, B. *et al.* Complete human day 14 post-implantation embryo models from naive ES cells. *Nature
1437* **622**, 562-573 (2023).

1438 222 Zhang, X.-z. *et al.* Folic Acid Rescues Valproic Acid-Induced Morphogenesis Inhibition in Neural
1439 Rosettes Derived From Human Pluripotent Stem Cells. *Frontiers in Cellular Neuroscience* **16** (2022).

1440 223 Sahakyan, V. *et al.* Folic Acid Exposure Rescues Spina Bifida Aperta Phenotypes in Human Induced
1441 Pluripotent Stem Cell Model. *Scientific Reports* **8**, 2942 (2018).

1442 224 Birtele, M. *et al.* Non-synaptic function of the autism spectrum disorder-associated gene SYNGAP1 in
1443 cortical neurogenesis. *Nature Neuroscience* **26**, 2090-2103 (2023).

1444 225 Hyun, I., Munsie, M., Pera, M. F., Rivron, N. C. & Rossant, J. Toward Guidelines for Research on
1445 Human Embryo Models Formed from Stem Cells. *Stem Cell Reports* **14**, 169-174 (2020).

1446 226 Blasimme, A. & Sugarman, J. Human stem cell-derived embryo models: Toward ethically appropriate
1447 regulations and policies. *Cell Stem Cell* **30**, 1008-1012 (2023).

1448 **KEY POINTS**

1449 • Stem cell-based embryo models can recapitulate essential developmental processes such as tissue
1450 patterning and morphogenetic events from pre-implantation to early organogenesis.

1451 • Bioengineering approaches, which are efficient in controlling tissue geometrical boundaries and
1452 interactions, chemical gradients and extracellular matrix signals, are instrumental to improve the
1453 efficiency and fidelity of stem cell-based embryo modeling.

1454 • Synthetic biology offers attractive approaches orthogonal to other bioengineering approaches to
1455 achieve programmable cellular complexity, architecture and function in bioengineered embryo
1456 models.

1457 • Bioengineered embryo models with enhanced efficiency, controllability, reproducibility,
1458 scalability and usefulness hold promise in fundamental research and biomedical applications.

1460 **Table 1. Stem cell-based embryo models discussed in the paper.**

1461 **Cell lineages:** EPI, epiblast. TE, trophectoderm. PrE, primitive endoderm. ExE, extraembryonic
 1462 ectoderm. VE, visceral endoderm. AVE, anterior visceral endoderm. PGC, primordial germ cell. NP,
 1463 neural plate. NPB, neural plate border. NNE, non-neural ectoderm.

1464 **Stem cells:** (mouse) mESC, mouse embryonic stem cell. mTSC, mouse trophoblast stem cell. mXEN,
 1465 mouse extraembryonic endoderm stem cell. mEPSC, mouse extended / expanded potential stem cell.
 1466 iGata4 mESC, mESCs transiently expressing *Gata4*. iCdx2 mESC, mESCs transiently expressing *Cdx2*.
 1467 (human) hPSC, human pluripotent stem cell. hEPSC, human extended / expanded potential stem cell.
 1468 iGATA6 hPSC, hPSCs transiently expressing *GATA6*. iGATA6-SOX17 hPSC, hPSCs transiently
 1469 expressing *GATA6* and *SOX17*. iGATA3-TFAP2C hPSC, hPSCs transiently expressing *GATA3* and
 1470 *TFAP2C*.

1471 **Embryo model names:** ETS embryoid, ESC-, TSC-derived embryo model. ETX embryoid, ESC-,
 1472 TSC-, XEN-derived embryo model. PASE, post-implantation amniotic sac embryoid. SEM, post-
 1473 implantation stem-cell-based embryo model. μNTLS, microfluidic neural tube-like structure. μSDM,
 1474 microfluidic somite development model.

| Mouse embryo models | | | | | |
|---------------------|--|-------------------------------|---|---|-------|
| Model names | Starting cell population | Approach | Developmental events modeled | Limitations | Ref. |
| Blastoid | mESC + mTSC; mEPSC; mEPSC + mTSC | Cell aggregation in microwell | Blastocyst formation; TE, EPI and PrE lineage segregation | Underdeveloped PrE; Limited developmental potential | 53-55 |
| ETS embryoid | mESC + mTSC | Cell aggregation in microwell | Post-implantation ExE and EPI compartment formation; EPI patterning | Low efficiency; Lack of VE | 71 |

| | | | | | |
|------------------------------|---|---|---|---|-----------|
| ETX embryoid | mESC + mTSC + mXEN; mESC + mTSC + <i>iGata4</i> mESC | Cell aggregation in microwell | Post-implantation ExE, VE and EPI compartment formation; AVE and A-P axis formation; Initiation of EMT and gastrulation | Low efficiency | 72,73,204 |
| Advanced ETX embryoid | mESC + mTSC + <i>iGata4</i> mESC; mESC + <i>iCdx2</i> mESC + <i>iGata4</i> mESC | Cell aggregation in microwell; <i>Ex utero</i> roller culture system | Post-implantation development up to neurulation and early organogenesis | Low efficiency; Structural defects in organ primordia | 75-77 |
| EpiTS embryoid | mESC + mTSC | Assembloid | Post-implantation EPI symmetry breaking and initiation of EMT | Lack of <i>in vivo</i> -like tissue morphology | 78 |
| Peri-gastrulation assembloid | mESC + BMP4-treated mESC | Assembloid | Post-implantation A-P and D-V patterned three germ layer derivatives | Lack of forebrain; Limited morphogenesis; Structural defects in organ primordia | 31 |
| Gastruloid | mESC | Cell aggregation in microwell | Post-implantation A-P patterning of germ layer lineages; Axial elongation | Limited morphogenetic events | 144 |
| Gastruloid with ECM | mESC | Cell aggregation in microwell; Matrikel embedding | Post-implantation A-P patterning of germ layer lineages; Axial elongation; Somite formation | Low efficiency | 139 |
| D-V patterned neural cyst | mESC | Matrikel embedding; Synthetic hydrogel | Spinal cord D-V patterning | Low efficiency; Lack of control of biochemical gradients | 99,101 |
| Trunk-like structure | mESC | Cell aggregation in microwell; Matrikel embedding | Post-implantation A-P patterning of germ layer lineages; Axial elongation; Somite and neural tube co-development | Lack of control of biochemical gradients | 141 |

| Human embryo models | | | | | |
|-----------------------------------|---|--|---|---|----------------|
| Model names | Starting cell population | Approach | Developmental events modeled | Limitations | Ref. |
| Blastoid | Naïve hPSC; hEPSC; Fibroblast reprogramming intermediate | Cell aggregation in microwell | Blastocyst formation; TE, EPI and PrE lineage segregation | Underdeveloped PrE; Limited developmental potential | 24,56,58-61,85 |
| PASE | Primed hPSC | Microfluidics | Post-implantation amnion-EPI patterning; PGC development; Initiation of EMT and gastrulation | Lack of A-P patterning in EPI | 32,83 |
| heX embryoid | Primed hPSC + <i>iGATA6</i> hPSC | Co-culture | Post-implantation amnion-EPI patterning; Bilaminar disc; A-P patterning of EPI; York sac formation; Haematopoiesis | Unclear identity of <i>iGATA6</i> hPSCs; Limited development of embryonic germ layers | 86 |
| Bilaminoid | Naïve hPSC + <i>iGATA6</i> hPSC | Cell aggregation in microwell | Post-implantation amnion-EPI patterning; Bilaminar disc; A-P patterning of EPI | Low efficiency | 91 |
| Extra-embryoid | hPSC with intermediate pluripotency | Cell aggregation in microwell | EPI and hypoblast segregation; Amnion-EPI patterning; A-P patterning of EPI | Low A-P patterning efficiency | 89 |
| Inducible embryoid | Naïve hPSC + <i>iGATA6-SOX17</i> hPSC + <i>iGATA3-TFAP2C</i> hPSC | Cell aggregation in microwell | Post-implantation amnion-EPI patterning; A-P patterning of EPI; PGC specification | Low efficiency; Lack of yolk sac-like structure | 90 |
| Peri-gastruloid | hEPSC | Cell aggregation in microwell | Bilaminar disc; Amnion-EPI patterning; A-P patterning of EPI; Initiation of EMT and gastrulation; PGC specification; Yolk sac formation | Low efficiency | 87 |
| SEM | Naïve hPSC + chemically induced PrE- and trophoblast-like cells | Cell aggregation in microwell; <i>Ex utero</i> roller culture system | Bilaminar disc; Amnion-EPI patterning; A-P patterning of EPI; PGC specification; Yolk sac formation; Development of ExEM and TE lineage | Low efficiency | 88 |
| 2D gastrulation model | Primed hPSC | Micropattern | Patterning of three germ layer lineages | Limited morphogenetic events | 25 |
| 2D gastrulation model on soft gel | Primed hPSC | Micropattern; Synthetic hydrogel | EMT and mesoderm ingestion | Limited germ layer patterning | 150 |
| Gastruloid | Primed hPSC | Cell aggregation in microwell | A-P patterning of germ layer lineages; Axial elongation | Limited morphogenetic events | 145 |

| | | | | | |
|---------------------------------|-------------|---|---|--|--------------------|
| 2D neural rosette | Primed hPSC | Micropattern | Neural tube morphology | Limited cell fate patterning or morphogenetic events | ^{191,195} |
| 2D ectoderm model | Primed hPSC | Micropattern | NP and NPB patterning | Limited morphogenetic events; Lack of NNE | ¹¹³ |
| | Primed hPSC | Micropattern | Ectoderm patterning | Limited morphogenetic events | ¹⁶⁶ |
| | Primed hPSC | Micropattern | Ectoderm patterning; neural cyst formation | Limited morphogenetic events | ¹⁶⁷ |
| Cranial neurulation model | Primed hPSC | Micropattern; Matrigel embedding | Cranial neural tube folding and closure | Lack of A-P or D-V axis | ¹⁴⁰ |
| Spinal cord neurulation model | Primed hPSC | Cell aggregation in microwell | Spinal cord neural tube folding and closure | Heterogeneity; Lack of D-V axis | ¹⁶⁸ |
| D-V patterned neural cyst | Primed hPSC | Matrigel embedding; Synthetic hydrogel | Spinal cord D-V patterning | Low efficiency; Lack of control of biochemical gradients | ¹⁰⁰ |
| A-P patterned neural tube model | Primed hPSC | Microfluidics | Brain region A-P patterning | Lack of 3D tubular morphology; Lack of D-V axis | ³³ |
| μ NTLS | Primed hPSC | Microfluidics | Neural tube A-P and D-V patterning | Lack of neural tube folding morphogenesis | ³⁴ |
| Somitoid | Primed hPSC | 2D culture of spheroids | Somitogenesis | Lack of sequential formation and A-P patterning of somites | ¹⁷⁷ |
| Segmentoid | Primed hPSC | Cell aggregation in microwell; Matrigel embedding | Axial elongation; A-P patterning; Somitogenesis | Lack of control of biochemical gradients | ¹⁷⁷ |
| Axioloid | Primed hPSC | Cell aggregation in microwell; Matrigel embedding | Axial elongation; A-P patterning; Somitogenesis | Lack of control of biochemical gradients | ¹⁷⁸ |
| μ SDM | Primed hPSC | Microfluidics; Matrigel embedding | Somitogenesis | Lack of sequential formation and A-P patterning of somites | ¹⁷⁹ |
| Trunk-like structure | Primed hPSC | Cell aggregation in microwell; Matrigel embedding | Axial elongation; A-P patterning; Somite and neural tube co-development | Lack of control of biochemical gradients | ¹⁸⁰ |

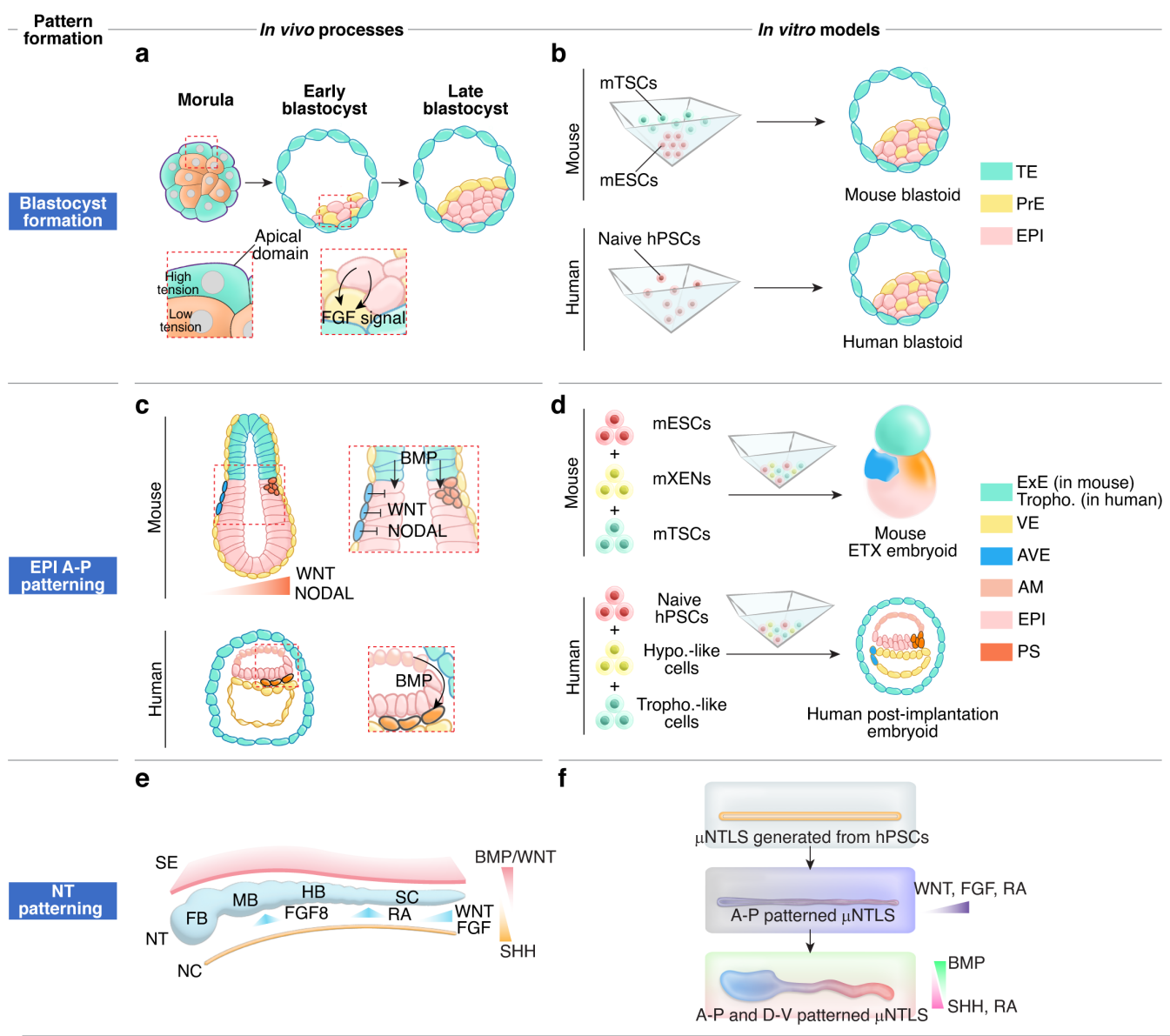
FIGURES AND FIGURE CAPTIONS**Figure 1**

Figure 1. Pattern formation *in vivo* and in embryo models. *In vivo* knowledge and *in vitro* modeling of blastocyst formation (a&b), epiblast symmetry breaking at the onset of gastrulation (c&d), and NT regional patterning (e&f). (a) Formation of mouse and human blastocysts as a self-organized pattern formation process, involving two rounds of cell lineage specification. The first cell fate decision leads to lineage segregation between TE and ICM. ICM cells then become segregated into EPI and PrE (or

1486 hypoblast in humans), a process that is suspected to be regulated by FGF signaling. **(b)** Aggregation and
1487 self-organization of mouse or human stem cells leads to the formation of mouse or human blastoids,
1488 respectively^{24,53-56,58,60,61}. **(c)** After blastocyst implantation, mouse embryo develops into an elongated
1489 structure with a cup-shaped EPI juxtaposed to ExE, surrounded by VE. In contrast, post-implantation
1490 human EPI exhibits a disc-like morphology, and it is juxtaposed with AM and hypoblast. Gastrulation is
1491 initiated in posterior EPI. Symmetry breaking and AP patterning of mouse EPI are guided by
1492 extraembryonic tissues. Similar mechanisms might be conserved in human gastrulation. **(d)** Aggregation
1493 of mouse or human embryonic and extraembryonic cells leads to mouse or human peri-gastrulation
1494 embryo models, respectively, recapitulating embryo morphology and A-P patterning of the EPI^{72,88}. **(e)**
1495 NT patterning *via* external morphogen gradients. A-P patterning of NT is mainly governed by WNT, RA
1496 and FGF signal gradients. D-V patterning of NT is mediated by BMP / WNT and SHH gradients
1497 secreted by SE and NC, respectively. **(f)** An A-P and D-V patterned NT model is achieved by exposing
1498 hPSC-derived tubular structures to stepwise orthogonal morphogen gradients³⁴. Cell lineages: TE,
1499 trophectoderm; PrE, primitive endoderm; EPI, epiblast; ExE, extraembryonic ectoderm; Tropho.,
1500 trophoblast; Hypo., hypoblast; VE, visceral endoderm; AVE, anterior visceral endoderm; AM, amnion;
1501 PS, primitive streak; NT, neural tube; FB, forebrain; MB, midbrain; HB, hindbrain; SC, spinal cord; SE,
1502 surface ectoderm; NC, notochord. Stem cells: mESCs, mouse embryonic stem cells; mTSCs, mouse
1503 trophoblast stem cells; mXENs, mouse extraembryonic endoderm stem cells; hPSCs, human pluripotent
1504 stem cells. Embryo model names: ETX embryoid, ESC-, TSC-, XEN cell-derived embryo models;
1505 μ NTLS, microfluidic neural tube-like structures. Others: A-P, anterior-posterior; D-V, dorsal-ventral;
1506 BMP, bone morphogenetic protein; FGF, fibroblast growth factor; RA, retinoic acid; SHH, sonic
1507 hedgehog.

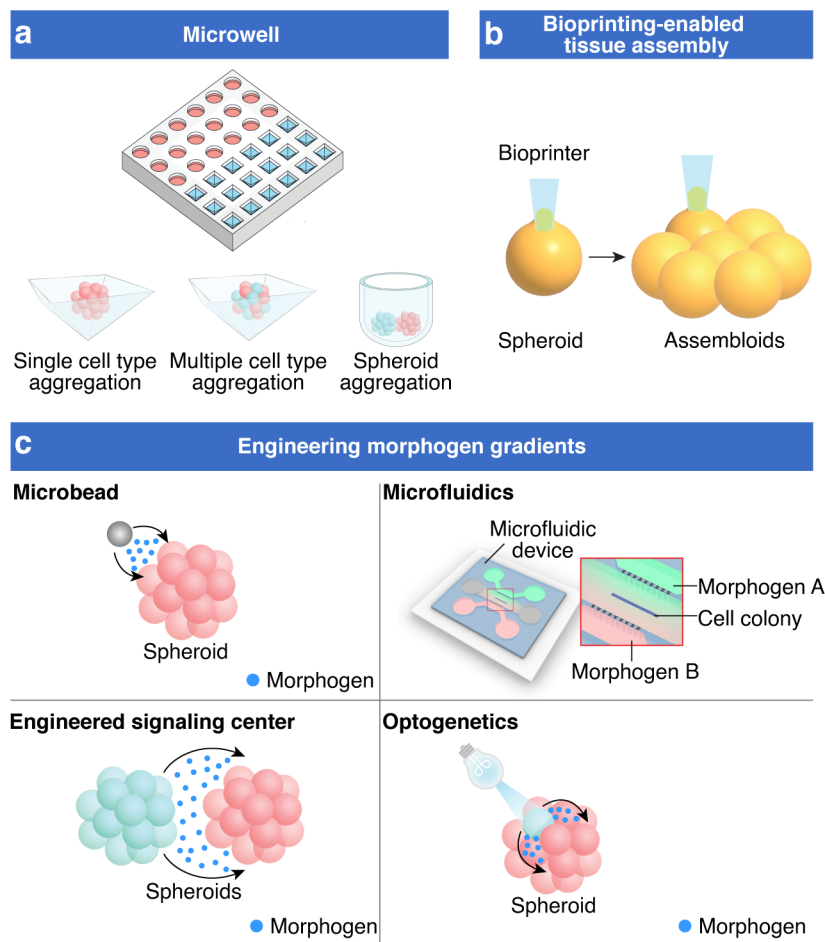
Figure 2

Figure 2. Bioengineering approaches for guiding pattern formation in embryo models. (a)

Microwells to promote cell and spheroid aggregation. **(b)** 3D bioprinting to assemble spheroids into

complex structures. **(c)** Engineering signaling centers and morphogen gradients through porous

microbeads, optogenetics, engineered signaling centers, and microfluidics, as indicated.

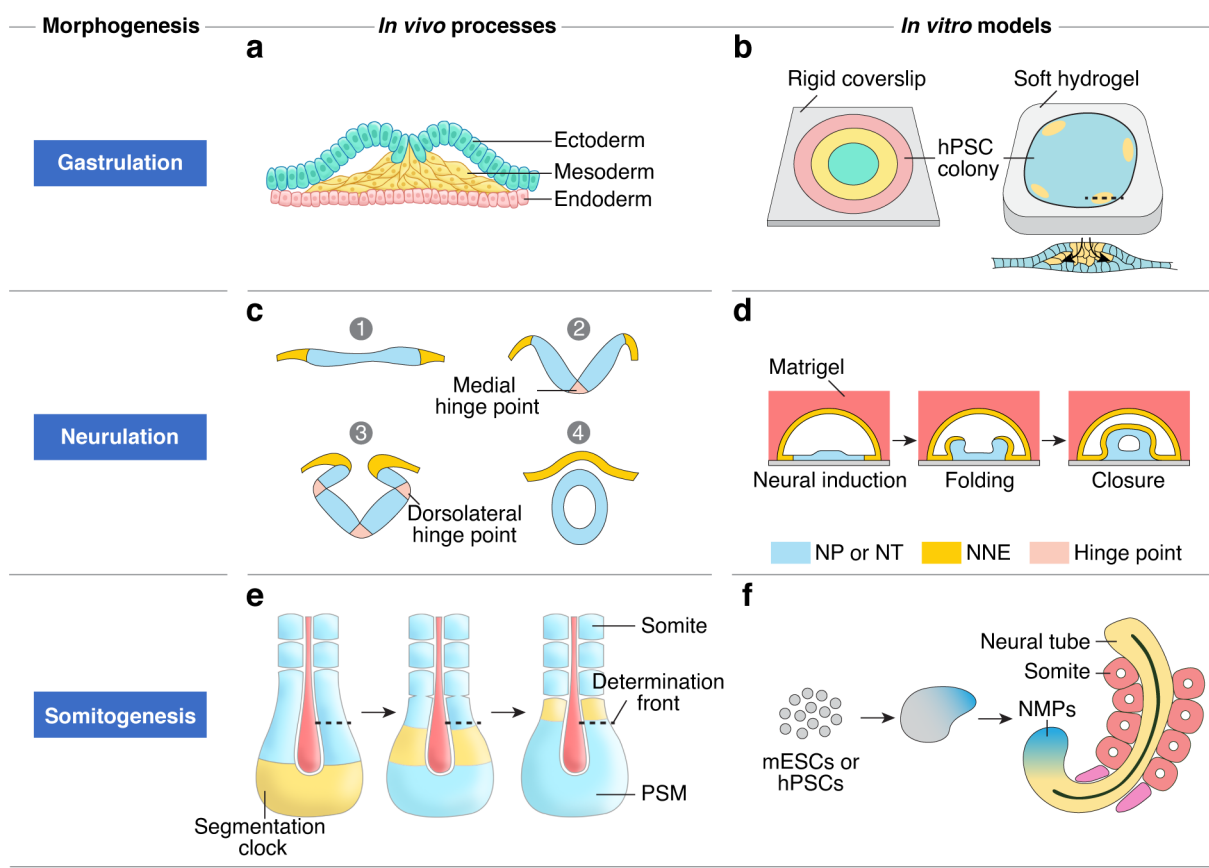
Figure 3.

Figure 3. Morphogenesis *in vivo* and in embryo models. *In vivo* knowledge and *in vitro* modelling of gastrulation (a&b), neurulation (c&d), and somitogenesis (e&f). (a) Gastrulation involves different morphogenetic events, such as EMT, cell migration and axial elongation, to organize the topology of three embryonic germ layers. (b) 2D micropatterned hPSC colonies treated with BMP4 develop into concentric rings of three germ layers, recapitulating cell fate patterning during gastrulation²⁵. Culturing micropatterned 2D gastrulation models on a soft hydrogel promotes gastrulation-like morphogenesis, such as ingestion and migration of mesoderm cells¹⁵⁰. (c) Bending and closure of the NP during neurulation. NP bending is primarily driven by mechanical forces generated by apical constriction in NP cells at the median and dorsolateral hinge points. (d) A neurulation model established by combining micropatterned 2D hPSC colonies with 3D culture to recapitulate NP folding and closure¹⁴⁰. (e) Somite

1528 formation during somitogenesis, which can be explained by the clock-and-wavefront model. In this
1529 model, somitogenesis is regulated by the combined action of a molecular segmentation clock and a
1530 moving determination front of FGF and WNT signaling activities. (f) Co-morphogenesis of NT- and
1531 somite-like structures in mouse or human embryo models^{141,180}. NP, neural plate. NT, neural tube. PSM,
1532 presomitic mesoderm. NMPs, neuromesodermal progenitors. mESCs, mouse embryonic stem cells.
1533 hPSCs, human pluripotent stem cells.
1534

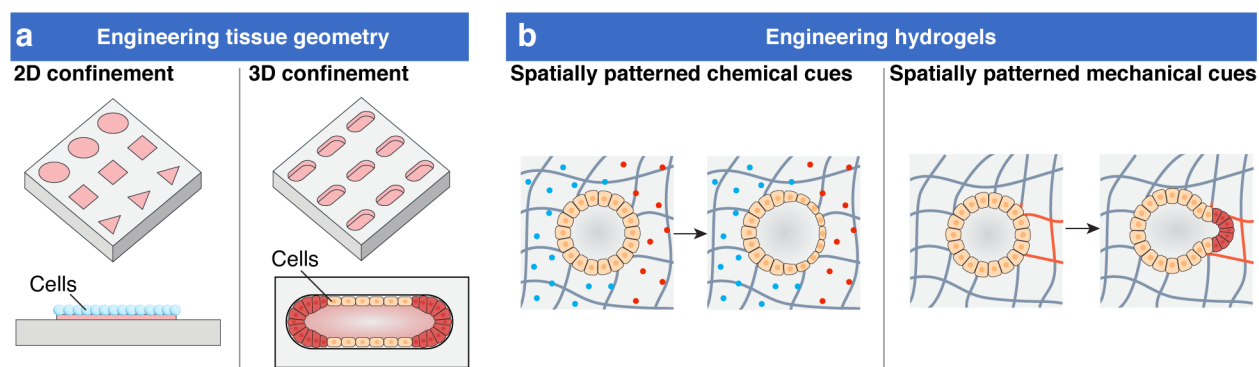
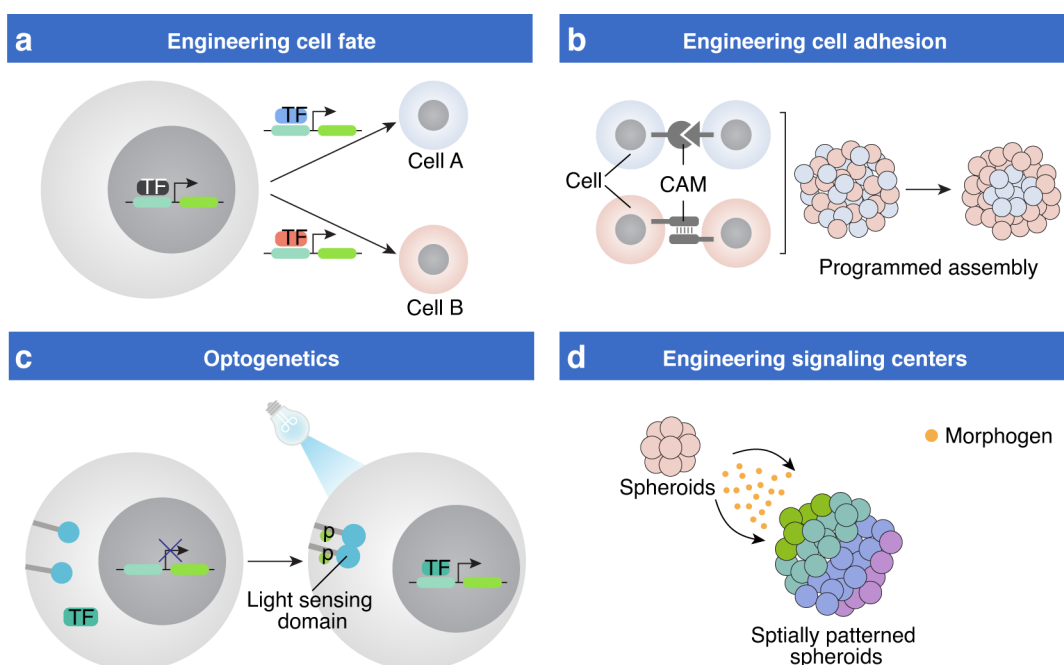
Figure 4

Figure 4. Bioengineering approaches to guide morphogenesis in embryo models. (a) Engineering

tissue geometry and boundary using micropatterning tools. (b) Synthetic hydrogels with engineered

spatially patterned chemical and mechanical cues.

1540

Figure 5.

1541

1542

Figure 5. Engineering cell behaviors using synthetic biology. (a) Engineering cell fate by controlling transcription factor expression to produce specific cell lineages. (b) Engineering cell adhesion using synthetic receptors, allowing programmed generation of spatially patterned multicellular structures²⁰⁹. (c) Optogenetics to modulate intracellular signaling pathways, for example, through fusing a light sensing domain with ligand receptors. (d) Engineering signaling centers to regulate fate specification and tissue patterning. Localized signaling centers can be generated by genetically engineering cells to express signaling molecules, which will guide spatial patterning of adjacent spheroids. Different colors represent different cell types. TF, transcription factor. CAM, cell adhesion molecule.

1550

1551

1552 **BOX 1. Applications of embryo models.**

1553 Stem cell-based embryo models provide an accessible and experimentally tractable approach to study
1554 mammalian development. Together with genome editing, live-cell imaging and multi-omics, stem cell-
1555 based embryo models are becoming attractive tools to elucidate molecular and cellular mechanisms in
1556 mammalian development. For example, owing to its controllability and compatibility with live-cell
1557 imaging, the microfluidic PASE model has been used to unveil a human-specific role of amniotic cells
1558 in triggering gastrulation-like events³². Pre-implantation embryo models, such as blastoids, highlight the
1559 important role of the interactions between embryonic and extraembryonic tissues, and could serve as a
1560 useful tool to study pregnancy loss arising from defects in embryonic-extraembryonic interactions.
1561 Recently, a co-culture system of human blastoids with endometrial organoids provides a valuable
1562 platform to study human implantation and understand implantation failure⁶². When combined with
1563 patient-derived hPSCs and genome-editing technologies, human embryo models could potentially
1564 provide novel insights into pathological conditions. For example, studies using neural rosettes have
1565 identified the roles of autism risk genes in early human neural development²²⁴. Embryo models have
1566 also been used to study the embryonic origin of late-onset neurodegenerative diseases, such as
1567 Huntington's disease¹⁶⁷. Finally, bioengineered embryo models, with enhanced efficiency,
1568 reproducibility and scalability, could potentially be applied in high-throughput teratogenicity and drug
1569 screens. Together, stem cell-based embryo models hold promise for advancing fundamental research in
1570 developmental and reproductive biology, as well as in biomedical applications for preventing and
1571 treating pregnancy loss, birth defects and developmental disorders.

1572

1573 **BOX 2. Ethical considerations of embryo models.**

1574 The similarity of stem cell-based embryo models to natural embryos, especially human ones, raises
1575 ethical concerns. In most countries, stem cell-based embryo models currently do not explicitly fit into
1576 existing legal regulatory categories. Historically, scientific societies such as the International Society for
1577 Stem Cell Research (ISSCR) have played a significant role in establishing ethical frameworks for stem
1578 cell research. ISSCR provided updated ethical guidelines for stem cell research in 2021²²⁰, which
1579 included considerations on embryo modelling research. ISSCR proposed that integrated embryo models
1580 should require stricter oversight than non-integrated ones. ISSCR guidelines also proposed prohibiting
1581 the transfer of human embryo models into any uterus or the use of human embryo models for
1582 reproduction purposes. Although none of the current embryo models are considered equivalent to human
1583 embryos or have shown the potential to develop into fetuses, as this field progresses further, embryo
1584 models are expected to mimic the entire natural embryo, or a considerable portion thereof, more closely
1585 in terms of molecular signatures, tissue structures, and development potential. Such similarity between
1586 human embryo models and natural ones inevitably raises ethical concerns. What should the legal
1587 definition of human embryos be? At what point should human embryo models be regulated as natural
1588 ones? There are ongoing discussions on these important questions, and readers are referred to other
1589 recent excellent reviews^{219,225,226}. Many scientists working in the field agree that for different scientific
1590 studies or biomedical applications, the least ethically challenging embryo models should be used. For
1591 example, while studying how the whole complex embryo develops might require integrated embryo
1592 models, studies of individual germ layer development or the formation of specific organs likely do not
1593 need the use of integrated embryo models. Another consideration is that there are many ethically less
1594 challenging, non-integrated embryo models available that mimic some aspects of human development,
1595 including gastrulation and early organ formation. These non-integrated embryo models are easier to
1596 study since they contain clearly defined cell types, with the cells organized into regular patterns, unlike

1597 the often-disorganized tissues found in most current integrated models. Since non-integrated embryo
1598 models are often built using bioengineering tools, they often are more efficient, reproducible and
1599 scalable. Continuous development of human embryo models calls for public conversations on the
1600 scientific significance of such research, as well as on the societal and ethical issues it raises.

1601

1602

1603 **SHORT SUMMARY (40 words)**

1604 Stem cell-based embryo models hold great promise to advance fundamental research and reproductive
1605 and regenerative medicine. This review discusses how bioengineering approaches can be utilized to
1606 construct embryo models with enhanced efficiency, controllability, reproducibility, scalability and
1607 usefulness.